Thermalization of topological entropy after a quantum quench

Yu Zeng,[1] Alioscia Hamma,[2,*] and Heng Fan[1]
[1]*Institute of Physics, Chinese Academy of Sciences, Beijing 100190, China*
[2]*Center for Quantum Information, Institute for Interdisciplinary Information Sciences, Tsinghua University, Beijing 100084, China*
(Received 25 November 2015; revised manuscript received 17 August 2016; published 2 September 2016)

Topologically ordered quantum phases are robust in the sense that perturbations in the Hamiltonian of the system will not change the topological nature of the ground-state wave function. However, in order to exploit topological order for applications such as self-correcting quantum memories and information processing, these states need to be also robust both dynamically and at finite temperature in the presence of an environment. It is well known that systems like the toric code in two spatial dimensions are fragile in temperature. In this paper, we show a completely analytic treatment of the toric code away from equilibrium, after a quantum quench of the system Hamiltonian. We show that, despite being subject to unitary evolution (and at zero temperature), the long-time behavior of the topological entropy is thermal, therefore vanishing. If the quench preserves a local gauge structure, there is a residual long-lived topological entropy. This also is the thermal behavior in presence of such gauge constraints. The result is obtained by studying the time evolution of the topological 2-Rényi entropy in a fully analytical, exact way.

DOI: 10.1103/PhysRevB.94.125104

I. INTRODUCTION

The development of quantum many-body physics in recent years has opened the doors—both theoretically and experimentally—to the exploration of new quantum phases of the matter [1,2] and the behavior away from equilibrium of quantum systems with many particles [3–6].

Novel quantum phases of matter that feature quantum or topological order (TO) cannot be described by the usual theory of symmetry and symmetry breaking and therefore are not characterized by a local order parameter [2,7–10]. They possess topological degrees of freedom and excitations described by a topological quantum field theory [11]. Moreover, they possess a long-range pattern of entanglement dubbed topological entropy (TE) that serves as nonlocal order parameter for these phases [12–24]. The topological entropy is associated with both the existence of a robust qubit [25–27] and of anyonic excitations. These topological characteristics make these states robust against a model noise based on local interactions, as it is very reasonable for the environment. For this reason, they are believed to be of great advantage for the implementation of quantum information processing, a paradigm dubbed topological quantum computing (TQC) [11,28–31].

On the other hand, coherent quantum dynamics has recently become accessible to experimental inquiry and study, in systems realized by means of ultracold atom gases in optical lattices [3–5]. The flexibility in engineering interactions in optical lattices makes them a very interesting way to implement Hamiltonians featuring topological order. The dynamics is obtained through the protocol of quantum quench [32]. The Hamiltonian of the system $H(\lambda)$ depends smoothly on a set of external parameters λ that are easy to control, like some coupling strength or strength of external fields. The system is initially prepared in the ground state of $H(\lambda_0)$ for some value λ_0 of the external parameters that at time $t = 0$ are suddenly switched to the quench value λ_1. The initial state will then evolve unitarily by means of the evolution generated by $H(\lambda_1)$ [33–37].

The main goal of this paper is the study of the resilience of TO away from equilibrium. At equilibrium, TO is a property of the ground-state wave function of a Hamiltonian, here the toric code Hamiltonian H_{TC} [31]. If we apply a perturbation to this Hamiltonian, we get a new ground state. Is the new ground state still topologically ordered? If yes (for a certain range of the perturbation strength), then TO is the property of a whole phase. Now this is indeed the case. If we perturb H_{TC} with any local perturbation λV (that is, a Hamiltonian that is the sum of local operators each of norm smaller than $|\lambda|$), we still have TO within a finite value of λ, after which a quantum phase transition happens. So TO is robust under static perturbations of the Hamiltonian. This kind of robustness has been shown in a number of papers [17,24,38–46]. Moreover, the robustness under static perturbations has recently been amenable to numerical study on large systems using two-dimensional density-matrix renormalization group methods [47,48]. It has been found that regardless of how the system is perturbed, the topological phase is robust for some finite strength of the perturbation. This means not only that the gap is robust until a critical value is reached (this has also been proven analytically in some remarkable papers [49–51]), but also that all the topological features are robust. They are indeed properties of the phase. In particular, it has been shown that the TE is robust.

Static here means that we prepare the system in the ground state of the new Hamiltonian so that we are always at equilibrium, namely in the ground state. However, one can imagine a different scenario. We do prepare the system in the ground state of the toric code H_{TC}, but immediately after the Hamiltonian changes to the perturbed one. It is the scenario of a sudden quantum quench. The prepared state is no longer the ground state of the new Hamiltonian, and therefore it is a state away from equilibrium and will undergo unitary evolution under the new Hamiltonian. The question we ask is, therefore, will TO be present in the wave function away from

*ahamma@mail.tsinghua.edu.cn

equilibrium? As we can see, the two types of robustness are very different.

To answer this question, we study the time evolution of the TE in the toric code after a quantum quench. The motivation for this study is threefold. First of all, if TO should be robust against perturbations in the Hamiltonian, this has to hold also for time varying stray magnetic fields, which would place the system away from equilibrium. The second motivation comes from the general relationship between quench dynamics and thermalization in a closed quantum system. In recent years, there has been a flourishing of results (see, e.g., Refs. [52–57] and Ref. [6] for extended references) about the foundations of quantum statistical mechanics. It has been understood that, if dynamics is complex enough—which is a generic situation—then a closed quantum system will make local observables thermalize, as the rest of the system can act as a thermal bath for the subsystem, although everything is away from equilibrium. One has then to analyze whether nonlocal order parameters like the TE in topological phases also thermalize. Finally, this kind of study gives us a handle to deal with the problem of finite temperature from a different point of view. If one can show that a system is robust against a quantum quench, then this would hint to the fact that the system may display robustness also at finite temperature.

The main result of the paper is that TO after a quantum quench will equilibrate to the thermal value at finite temperature [58–61]. That is, zero if no symmetry is imposed or half of the initial value if the gauge structure is preserved. Therefore, in two dimensions (2D), TO in the toric code will not survive a quantum quench. It is important to realize that TO is destroyed even in the case of a small quench, when the evolving Hamiltonian still possesses TO, in the sense that its ground state is topologically ordered. In other words, static and dynamic perturbations have a very different effect, and while the TO in H_{TC} is robust under a static perturbation, a sudden quench will destroy it.

In dealing with the dynamics of a system with TO after a quantum quench there are several subtleties to consider. Generically, if the system dynamics is complex enough, every local subsystem can see the rest of the system as an environment and thermalize locally, in spite of the fact that the global evolution is unitary. However, topological order comes from the presence of a nonlocal order and nonlocal patter of entanglement. Therefore, local thermalization does not necessarily imply whether topological degrees of freedom or topological observables do indeed thermalize. After all, one of the goals of using topological states of the matter for quantum computation is to have some topological observables that do not decohere or thermalize while typical local observables will. So one cannot just borrow the local thermalization picture and draw conclusions. One needs to calculate. This issue has been explored in the past by some of us [62] and other authors [34,63,64]. The complexity of dealing with the time evolution of a quantum system, is, of course, formidable. Numerical analysis is limited to very small system sizes. In Ref. [65] it was indeed found that TO and TE would not survive certain quenches that would break the gauge symmetry, but because of very small system sizes the results were not conclusive. From the analytical side, previous results relied on the simplification stemming from the restriction to a gauge-preserving quench [62]. In this case, it was shown that the topological entropy computed from a subsystem with spins only on the boundary but no bulk, which we call a thin subsystem, in the 2D toric code is robust. In Ref. [34], the effect of the breaking of integrability was shown to be unable to create topological order, together with a volume law for entanglement, thus suggesting that quantum quenches would be like thermalization for the toric code.

In this paper, we attack the problem of a quantum quench of the 2D toric code without requiring that it preserves any symmetry of the system, including the gauge structure. We present a fully analytical solution of the problem by developing and extending to the time domain a technique presented in Ref. [66]. The technique also allows us to study the TE associated with a subsystem with a bulk instead of a thin subsystem. We show that the presence of the bulk is very important and that in the time evolution the difference between thin and thick subsystems is critical, whereas in the case of static perturbations both subsystems yield similar results. In order to perform a fully analytical treatment, we choose the quench so that the system is completely integrable in free fermions, dubbed the "τ picture" [67–69]. Let us here point out another subtle issue. One would think that if the evolving Hamiltonian is fully integrable, there should be no thermalization at all. Indeed, as a whole the system does not thermalize. There is an extensive number of conserved quantities in the so-called τ picture. However, that does not mean that *every* observable must not thermalize. Here we show that the TE will thermalize even after an integrable quench. We study the integrable quench in order to obtain a fully analytic solution. We see that in 2D topological properties like TE are even more fragile than local degrees of freedom. *A fortiori*, though, under a nonintegrable quench, no degree of freedom, topological or not, will be conserved. In order to apply these techniques in the nonintegrable case, one could resort to perturbation theory following the lines of Refs. [62,70]. Moreover, one can pair the same technique with numerical techniques to study systems with disorder.

II. TOPOLOGICAL RÉNYI ENTROPY AFTER A GAUGE-BREAKING QUANTUM QUENCH

We start with the toric code model (TCM) introduced by Kitaev [31]. The Hamiltonian for this model defined on a square lattice with $N \times N$ sites with spins-$\frac{1}{2}$ on the bonds is given by

$$H_{TC} = -\sum_s A_s - \sum_p B_p, \tag{1}$$

where the star operators $A_s \equiv \prod_{i\in s} \sigma_i^x$ and the plaquette operators $B_p \equiv \prod_{i\in p} \sigma_i^z$ belong to stars (s) and plaquettes (p) on the lattice containing four spins each (see Fig. 1). The total Hilbert space is the 2^{2N^2}-dimensional Hilbert space $\mathscr{H}$ of the spins on the bonds. Notice that the subspace $\mathscr{H}_{\text{gauge}} \subset \mathscr{H}$ obtained by projecting onto the subspace with all the $A_s = +1$ is the gauge invariant Hilbert space of the Z_2 quantum lattice gauge theory [2] whose dimension is 2^{N^2+1}. In the following, we say that the gauge structure or gauge symmetry is preserved if the perturbation commutes with all the A_s and therefore the system stays in the same space $\mathscr{H}_{\text{gauge}}$.

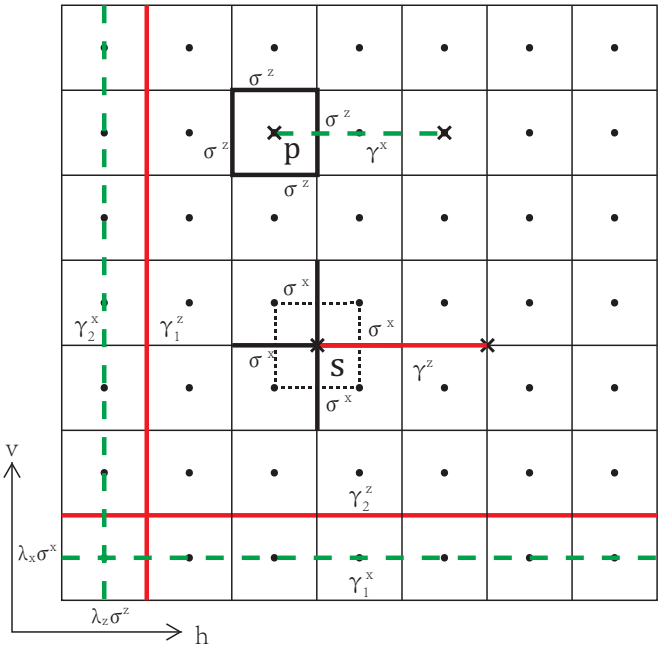

FIG. 1. A $N \times N$ square lattice with periodic boundary condition and spins-$\frac{1}{2}$ live on the edges. Examples of star operator located on lattice site (s) and the plaquette operator located on dual lattice site (p) are shown. There are two types of open strings corresponding to two types of excitations. It also shows the horizontal edges (along the direction h) and the vertical edges (along the direction v). We arrange fields in the $+z$ direction with magnitude of λ_z on the horizontal edges and fields in the $+x$ direction with λ_x on the vertical edges.

The model in Eq. (1) features topological order in the ground state. If we add a perturbation $V(\lambda)$ that is the sum of local operators, for a finite range of λ topological order is preserved [17,24,39,40,42–46]. On the other hand, if the system is put in contact with a heat reservoir and we wait for thermalization to happen (or if we do prepare the system in the Gibbs state), the topological order is destroyed. How do we detect topological order in a system? It is very remarkable that topological order is detected and consists in a particular pattern of entanglement in the wave function. Entanglement is the most defining property of quantum mechanics. If something is genuinely quantum, that is, it cannot be simulated or explained with just classical concepts, one needs to take in account entanglement [71,72]. For this reason, quantum order or quantum phases of matter must have some nontrivial patterns of entanglement [14,15], and a big part of the recent effort in condensed-matter theory and quantum field theory resides in the calculation of entanglement. However, as measured by the von Neumann entropy, entanglement is a formidable quantity to compute and measure. It requires the knowledge of all the eigenvalues of the reduced density matrix. So it requires perfect knowledge of the wave function, which is a very hard task from the analytical, numerical and experimental point of view. If one wants to use entanglement properties as an order parameter, one should look for quantities that are, in principle, measurable; that is, they are the expectation value of some Hermitian operator, and the Hermitian operator must not explicitly depend on the wave function itself. What choices do we have? We can consider the generalization of the von-Neumann entropy to a family of entropies known as α-Rényi entropies, defined as

$$S_\alpha^{AB} \equiv \frac{1}{1-\alpha} \log_2 \mathrm{Tr}\left[\rho_A^\alpha\right] \tag{2}$$

associated to the reduced density matrix $\rho_A = \mathrm{Tr}_B \rho$ after a tensor product structure of the Hilbert space $\mathscr{H} = \mathscr{H}_A \otimes \mathscr{H}_B$. In the case of $\alpha = 2$, though, we can find a very useful interpretation of the Rényi entropy,

$$S_2^{AB} = -\log_2 \mathrm{Tr}\left[\rho_A^2\right] = -\log_2 P, \tag{3}$$

where P is the purity of the state ρ_A. Now this quantity is a simple function of an observable. We need to first prepare two copies of $\rho \to \rho \otimes \rho \in (\mathscr{H}_A \otimes \mathscr{H}_B) \otimes (\mathscr{H}'_A \otimes \mathscr{H}'_B)$. Then, considering the two copies of ρ_A, namely $\rho_A^{\otimes 2}$, one has

$$P = \mathrm{Tr}\left[\rho_A^2\right] = \mathrm{Tr}[\mathbb{S}_A \rho^{\otimes 2}], \tag{4}$$

where $\mathbb{S}_A$ is the swap operator between the two copies of ρ_A [73]. Here is a simple proof. An arbitrary state ρ in $\mathscr{H}$ can be written as $\rho = \sum_{i_A i_B j_A j_B} \alpha^{i_A i_B}{}_{j_A j_B} |i_A, i_B\rangle\langle j_A, j_B|$, where $|i_A\rangle$ and $|i_B\rangle$ are the bases in $\mathscr{H}_A$ and $\mathscr{H}_B$, respectively. The coefficient $\alpha^{i_A i_B}{}_{j_A j_B}$ satisfies the Hermitian constraint $\alpha^{i_A i_B *}{}_{j_A j_B} = \alpha^{j_A j_B}{}_{i_A i_B}$ and normalization condition $\sum_{i_A i_B} \alpha^{i_A i_B}{}_{i_A i_B} = 1$. Actually, ρ is a tensor of type (2,2), and we use the Einstein summation convention for simplicity, namely, $\rho = \alpha^{i_A i_B}{}_{j_A j_B} |i_A, i_B\rangle\langle j_A, j_B|$. Then $\rho^{\otimes 2} = \alpha^{i_A i_B}{}_{j_A j_B} \alpha^{k_A k_B}{}_{l_A l_B} |i_A, i_B\rangle\langle j_A, j_B| \otimes |k_A, k_B\rangle\langle l_A, l_B|$. Note that $\mathbb{S}_A$ "swaps" the two copies' component in $\mathscr{H}_A$ and $\mathscr{H}'_A$ as $\mathbb{S}_A |i_A, i_B\rangle\langle j_A, j_B| \otimes |k_A, k_B\rangle\langle l_A, l_B| = |k_A, i_B\rangle\langle j_A, j_B| \otimes |i_A, k_B\rangle\langle l_A, l_B|$. In the end we calculate the trace and finally get $\mathrm{Tr}[\mathbb{S}_A \rho^{\otimes 2}] = \alpha^{i_A i_B}{}_{k_A i_B} \alpha^{k_A k_B}{}_{i_A k_B}$. We can see that the swap operator actually "swaps" the contraction indexes of the tensor. It is easy to verify that the result is the same when we calculate $\mathrm{Tr}[\rho_A^2]$. So the 2-Rényi entropy simply reads $S_2^{AB} = -\log_2 P = -\log_2 \mathrm{Tr}[\mathbb{S}_A \rho^{\otimes 2}]$.

Now, the von Neumann entropy is the unique measure of bipartite entanglement that quantifies [71,74] the conversion into Bell pairs that one can obtain from a state, which is important for quantum information processing protocols. However, as far as properties of the phase are concerned in condensed matter, the Rényi entropy is as good. It marks quantum phase transitions in the same way, and, when entanglement characterizes a phase, S_2^{AB} does it as well. In particular, it has been shown [75] that TE measured by the Rényi entropy detects TO in exactly the same way. The fact that the 2-Rényi entropy is the expectation value of an observable also makes it possible to conceive realistic scenarios for its measurement [76–79]. This is important as the search of quantities that can be measured for detecting topological order is one of the most important topics in the field. So the topological part of the 2-Rényi entropy is a possible candidate, together with other measures; see Refs. [80,81].

Following Refs. [14,15], the topological Rényi entropy is defined as the linear combination of four Rényi entropies associated with four different regions (1), (2), (3), and (4) (see Fig. 2):

$$S_\alpha^T \equiv -S_\alpha^{(1)} + S_\alpha^{(2)} + S_\alpha^{(3)} - S_\alpha^{(4)}. \tag{5}$$

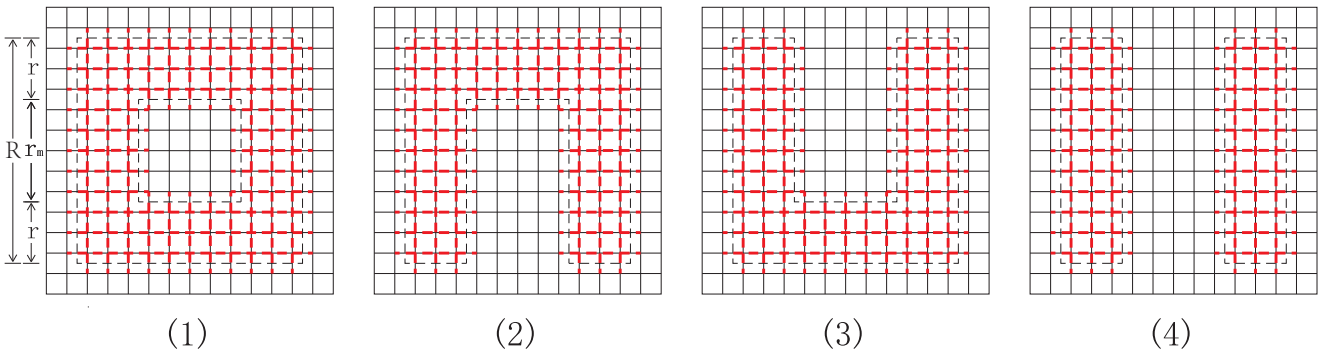

FIG. 2. Illustration of the subsystems A (red dashed lines) and B (black solid lines) in the four cases that are applied to calculate the topological entropy with extension $R = 11$ and thickness $r = 3$. $r_m = R - 2r$ is the side length of the "hole" belonging to the subsystem (1).

The size of the subsystem is characterized by two linear dimensions: the extension R and the thickness r. The size of the "hole" in the subsystem (1) is characterized by $r_m = R - 2r$.

For the toric code model H_{TC}, the topological entropy reads $S_\alpha^T = 2$, for every α [75]. As mentioned above, for a finite range of λ, the system stays in the topological phase, and accordingly, the value of $S_2^T(\lambda)$ in the new ground state of the Hamiltonian

$$H(\lambda) = -\sum_s A_s - \sum_p B_p + V(\lambda) \tag{6}$$

is preserved in the limit of $R,r,r_m \to \infty$ [17,24,39,40]. On the other hand, for every finite temperature β, the value of S^T in the thermal state $\rho = Z^{-1}e^{-\beta H_{TC}}$ goes to zero in the thermodynamic limit. However, if one freezes one of the series of quantum numbers A_s or B_p (i.e., if one enforces a gauge symmetry), the value of S^T goes to one half of the full value, namely $S^T(\text{gauge}) = 1$, signaling a classical form of topological order in the system [58–60].

In this paper, we want to understand the dynamics of S^T after a quantum quench. The protocol of the quantum quench is simple. We prepare the system in the state $\Psi(0)$ being in the ground state of H_{TC}, and then, at $t = 0$, we suddenly switch on the term $V(\lambda)$ in $H(\lambda)$. The wave function of the system will then evolve unitarily as

$$|\Psi(t)\rangle = e^{-iH(\lambda)t}|\Psi(0)\rangle. \tag{7}$$

Taking the trace over the degrees of freedom in B of the above state, we can obtain the time evolution $\rho_A(t)$ of the partial state. We set on studying the presence of topological order after a quantum quench by studying then the quantity $S_2^T(t) = S_2^T[\rho_A(t)]$. In order to find a fully analytical solution of this problem, we need to find a perturbation $V(\lambda)$ of the toric code such that the model is still completely integrable. In this way, one can study exactly both the ground-state manifold and the time evolution after a quantum quench as the perturbation $V(\lambda)$ is switched on [40,62]. Again, we want to highlight that using an integrable model is the right thing to do if one wants to prove fragility. If we found that TE is robust under an integrable quench, we could suspect that thermalization fails to happen just because of the many conserved quantities. However, if TE thermalizes under an integrable quench, it will thermalize even more so if the evolving Hamiltonian is nonintegrable. In particular, let us see how the toric code with a certain arrangement of the external fields can be mapped into a system of free fermions [66,82]. We write $V(\lambda)$ as the sum of external fields on the bonds, with a special arrangement: the field in the $+z$ direction with magnitude of λ_z on the horizontal (h) edges and the field in the $+x$ direction with λ_x on the vertical (v) edges. In this model, there are $2N^2$ spins on the edges of an $N \times N$ square lattice with periodic boundary conditions (see Fig. 1). The Hamiltonian for the model then reads

$$H(\lambda) = -\sum_s A_s - \sum_p B_p - \lambda_z \sum_{i\in h} \sigma_i^z - \lambda_x \sum_{i\in v} \sigma_i^x. \tag{8}$$

Notice that when one of the λ_x,λ_z is zero, the system preserves one of the two local $\mathbb{Z}_2$ gauge symmetries $[H(\lambda_z),B_p] = [H(\lambda_x),A_s] = 0$ for every s,p. One of the main goals of this paper is to find results when no gauge symmetry is imposed on the system, namely $\lambda_x \neq 0,\lambda_z \neq 0$. After exact diagonalization, one can obtain an analytic expression for $|\Psi(t)\rangle$. Moreover, one can calculate analytically all the many-spin correlation functions as a function of time. This is a key point to obtain what we want. Indeed, from the technical point of view, the main result is that we can compute the topological 2-Rényi entropy as a function of time t, and quench strengths $\lambda = (\lambda_x,\lambda_z)$ for the time evolution after a quantum quench, namely,

$$S_2^T(t,\lambda) = \log_2\left[\frac{P^{(1)}(t,\lambda)P^{(4)}(t,\lambda)}{P^{(2)}(t,\lambda)P^{(3)}(t,\lambda)}\right], \tag{9}$$

where $P(t,\lambda)$ is the purity of the evolved subsystem A, namely,

$$P(t) = \mathrm{Tr}_A\{\mathrm{Tr}_B[e^{-iH(\lambda)t}|\Psi(0)\rangle\langle\Psi(0)|e^{iH(\lambda)t}]\}^2. \tag{10}$$

The mapping into free fermions mentioned above proceeds from a first mapping of the physical spins on the links, which we call the "σ picture," to some effective spin on the sites, of both the initial lattice and the dual lattice (i.e., the sites of the plaquettes). This picture is called here the "τ picture," $H(\lambda)$. This mapping brings the model $H(\lambda)$ into the sum of the Ising chains in transverse field over $2N$ different lines, namely, N rows on the lattice, and N rows on the dual lattice. The eigenspace of $H(\lambda)$ in the τ picture is a tensor product over the different chains. At this point, we show that $P(t)$ can be calculated exactly by sum of correlation functions [62,66,83,84]. The details of the mapping and the solution in terms of correlation functions are shown in the Appendix.

The main result of this paper is obtaining a closed formula for the 2-Rényi topological entropy after a quantum quench. This is given by substituting the following expression for the purity of the state ρ_A into Eq. (10):

$$P(t) = C_P \sum_{\partial\tilde{g}\in\partial G'_A} \sum_{\substack{\tilde{g}\in G'_A \\ \tilde{z}\in Z_A}} |\langle \tilde{g}\partial\tilde{g}\tilde{z}\rangle_{\Psi(t)}|^2 \sum_{\substack{\tilde{h}\in H'_A \\ \tilde{x}\in X'_A}} |\langle \tilde{x}\partial\tilde{x}(\partial\tilde{g})\tilde{h}\rangle_{\Phi(t)}|^2 \times \sum_{\partial\bar{g}\in\partial G'_B} (-1)^{\partial\bar{g}\partial\bar{x}(\partial\bar{g})\cap\bar{z}\bar{h}}. \quad (11)$$

In the above formula, $\Psi(t)\otimes\Phi(t)$ describes the time evolution of the system (Ψ and Φ refer to the quantum numbers on two different sublattices: In Fig. 1, they correspond to the lattice and the dual lattice, respectively). The operators $\tilde{g},\tilde{z},\tilde{h},\tilde{x},\partial\tilde{g}\partial\tilde{x}(\partial\tilde{g})$ and $\partial\bar{g}\partial\bar{x}(\partial\bar{g})$ represent string operators operating with the Pauli algebra on the spins in the lattice, in either subsystem A or subsystem B. The phase factor takes into account whether such operators commute or anticommute. As we can see, the evaluation of this formula requires just the knowledge of correlation functions. As the system $H(\lambda)$ is integrable, all these quantities can be obtained analytically. Notice that for $t = 0$, this is the topological entropy in any given eigenstate of the system. The derivation of Eq. (11) is far from being trivial, and it requires several pages of calculations. The full derivation is presented in the Appendix, where it appears as Eq. (A54).

The formula Eq. (11) holds for every size N of the system and R,r for the subsystem. As one can see, though, the number of correlation functions to compute grows exponentially with the size of the subsystem A. For example, for a subsystem of the type (1) with R,r (see Fig. 2), the number of correlation functions to compute scales as 2^{2R+2r}. Each correlation function can be expressed as a Pfaffian; the computation of a Pfaffian can be reduced to the computation of a determinant whose maximum dimension is $2(R+1)$ [83,84]. Although the number of correlation functions to compute is exponential, this calculation can be effectively carried over also for large R,r by using parallelization on high performance computing clusters.

III. RESULTS AND DISCUSSION

In this section, we show the results obtained from the computation of Eqs. (9) and (11).

Let us first show the effect of a static perturbation. This amounts to compute Eq. (10) in the instantaneous ground state ($t = 0$) as λ is varied. In Fig. 3 we can see the effect of a

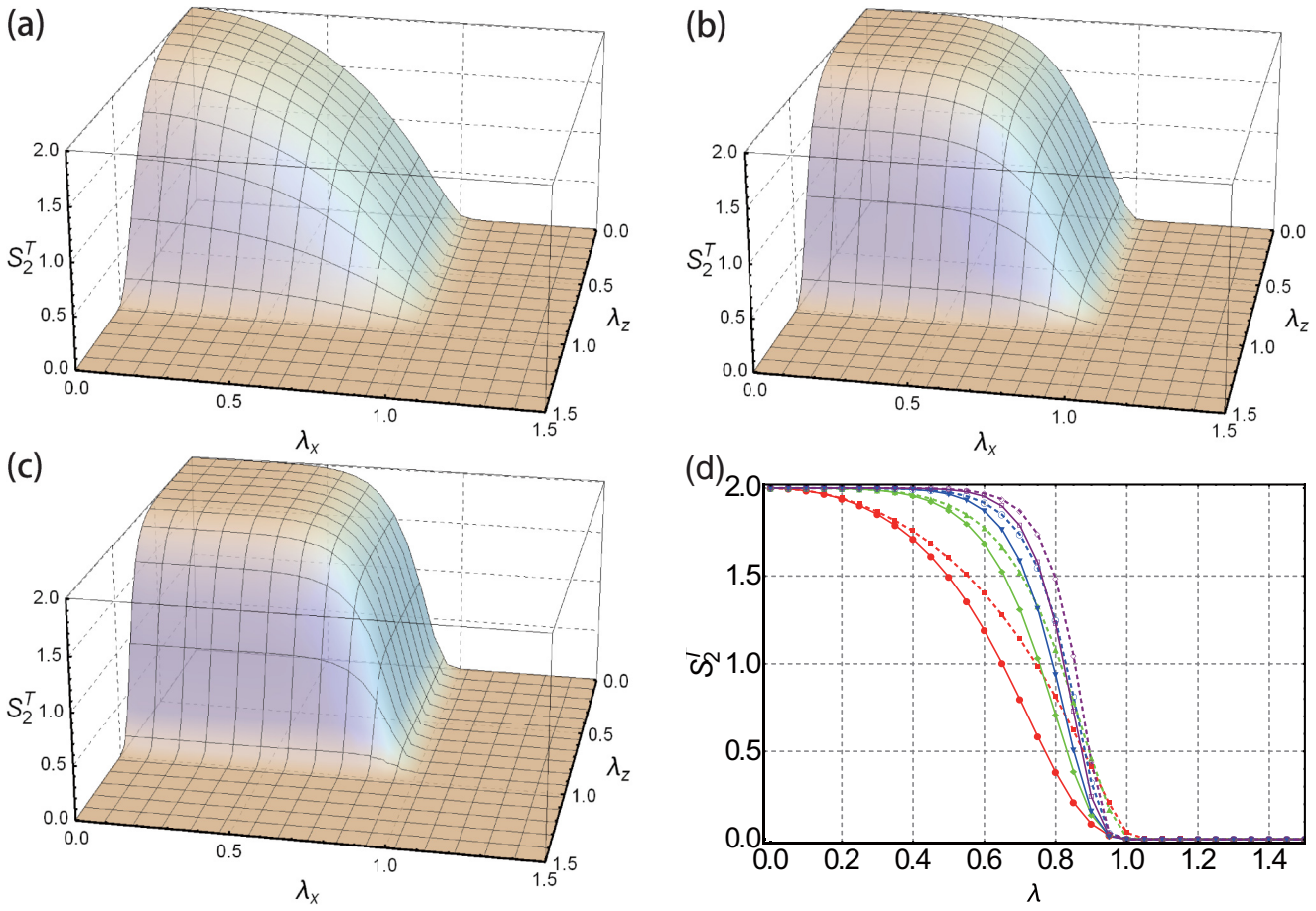

FIG. 3. Topological Rényi entropy S_2^T in static case as a function of fields λ_x and λ_z with different system sizes: (a) $R = 5$, $r = 1$, $N = 100$; (b) $R = 8$, $r = 2$, $N = 160$; (c) $R = 11$, $r = 3$, $N = 220$. (d) Illustration of S_2^T with Hamiltonian preserving Z_2 gauge symmetry ($\lambda_z = 0,\lambda_x = \lambda$, dashed lines) and breaking gauge symmetry ($\lambda_z = \lambda_x = \lambda$, solid lines). Various colors represent distinct system sizes: red, $R = 5$, $r = 1$, $N = 100$; green, $R = 8$, $r = 2$, $N = 160$; blue, $R = 11$, $r = 3$, $N = 220$; purple, $R = 14$, $r = 4$, $N = 280$.

perturbation in the ground state. After the critical point $\lambda = 1$, topological order is destroyed and TE vanishes. As the system size (both r and r_m) increases, the transition becomes sharper. As we can see, the presence of the gauge structure makes TO more resilient, and the TE vanishes in a smoother way. If gauge structure is destroyed, the transition is much sharper. The result in the presence of gauge symmetry is in complete accordance with earlier results [40], both numerical and analytical.

Of course, the main goal of this work is to show what happens for the time evolution. While static perturbations can be effectively studied by numerical methods, the time evolution is too complex to be effectively simulated numerically, and that is where an analytic treatment is needed. Moreover, we are interested in a generic quench such that every symmetry (including the gauge symmetry) can be destroyed. This is indeed the case as long as one of the λ_x,λ_z is nonvanishing.

In Fig. 4, we show the fate of TE measured by S_2^T in the thermodynamic limit $N \to \infty$ at infinite times $t \to \infty$ for different subsystem sizes R,r. The result is fully analytical. We see that, as gauge symmetry is broken, the TE vanishes in the limit of large subsystem size. Some residual TE survives for small subsystem sizes and moderate λ. However, as we discuss later, the value of λ such that S_2^T vanishes is pushed back as subsystem size increases. On the other hand, if the gauge symmetry is preserved (meaning either λ_z,$\lambda_x = 0$), then $S_2^T = 1$ for large subsystem sizes, which is half of the full value in the toric code. This is the main result of the paper: After a quantum quench, at large times the system has the same topological entropy as in the thermal state. As it was shown in Refs. [26,58,59,61], if gauge symmetry is present, then the thermal state possesses a classical topological order with half the value of the full topological entropy. This corresponds to the existence of a protected classical bit of information [26]. On the other hand, if no gauge symmetry is preserved, in the thermodynamic limit all the TE disappears, corresponding to no possible information stored in a protected way in the system [26]. Therefore, the main message is, *after a quantum quench, topological order thermalizes*. It is remarkable that this happens even when the quench is integrable. This means that even though the system does not fully thermalize, as there are many conserved local quantities, the evolution is complex enough to destroy the topological order and the topological

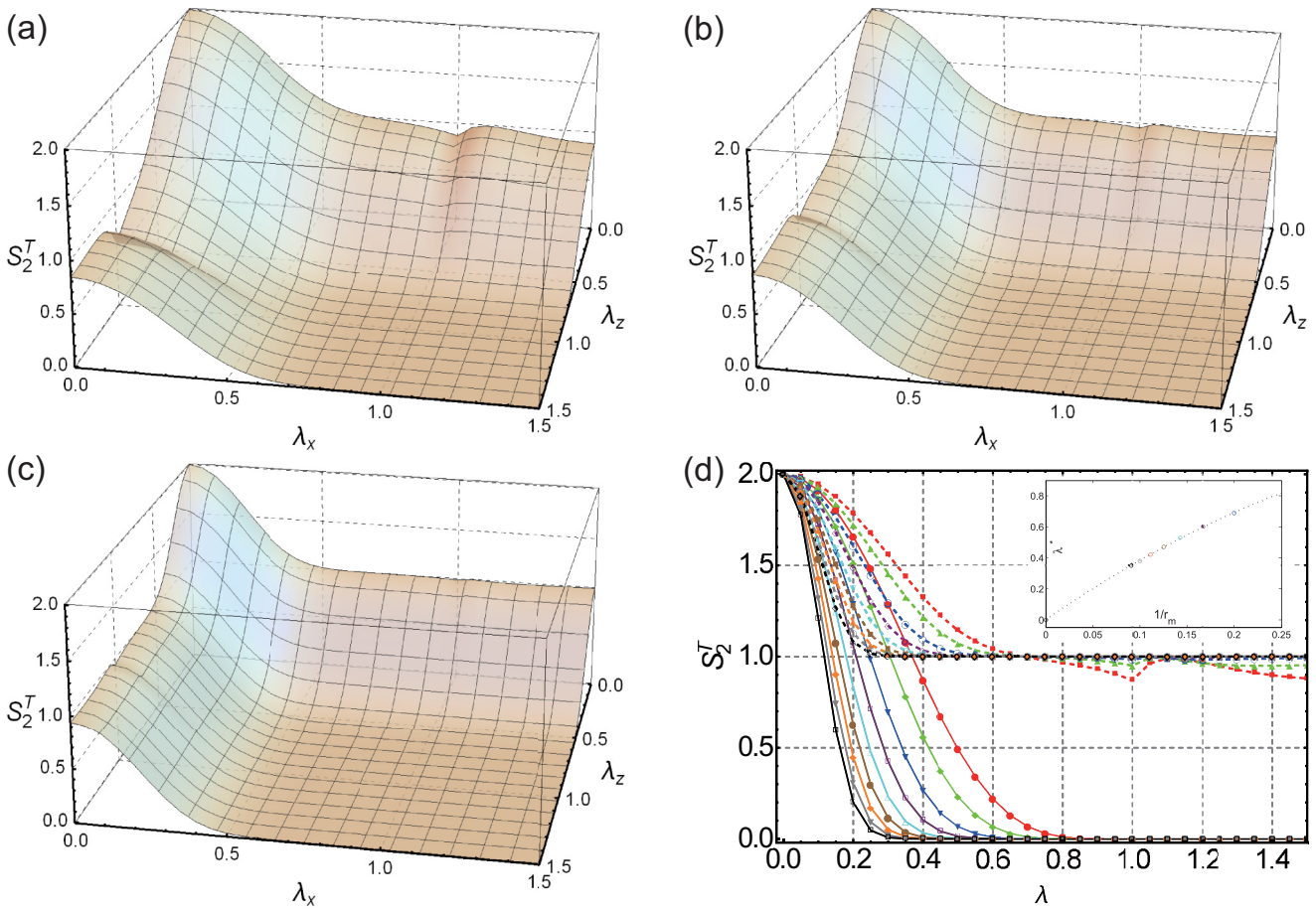

FIG. 4. Topological Rényi entropy S_2^T in the quantum quench case as a function of fields λ_x and λ_z with different subsystem sizes in thermodynamic limit ($N \to \infty$) and infinite time limit ($t \to \infty$): (a) $R = 5$, $r = 1$; (b) $R = 8$, $r = 2$; (c) $R = 11$, $r = 3$. (d) Illustration of S_2^T with quench Hamiltonian preserving Z_2 gauge symmetry ($\lambda_z = 0$, $\lambda_x = \lambda$, dashed lines) and breaking gauge symmetry ($\lambda_z = \lambda_x = \lambda$, solid lines). Various colors represent distinct subsystem sizes (r_m,R,r), where $r_m = R - 2r$. In quantum quench case, S_2^T, as a function of the subsystem size, depends mostly on r_m but is not sensitive to r: red (3,5,1); green (4,8,2); blue (5,11,3); purple (6,14,4); cyan (7,13,3); brown (8,14,3); orange (9,13,2); gray (10,14,2); black (11,15,2). Inset in panel (d): polynomial fit (dotted line) of λ^*, at which point $S_2^T(\lambda^*, t \to \infty) < \varepsilon$, as a function of $1/r_m$ with fixed $r = 2$. We sample r_m as (5, 6, 7, 8, 9, 10, 11) and choose $\varepsilon = 10^{-3}$.

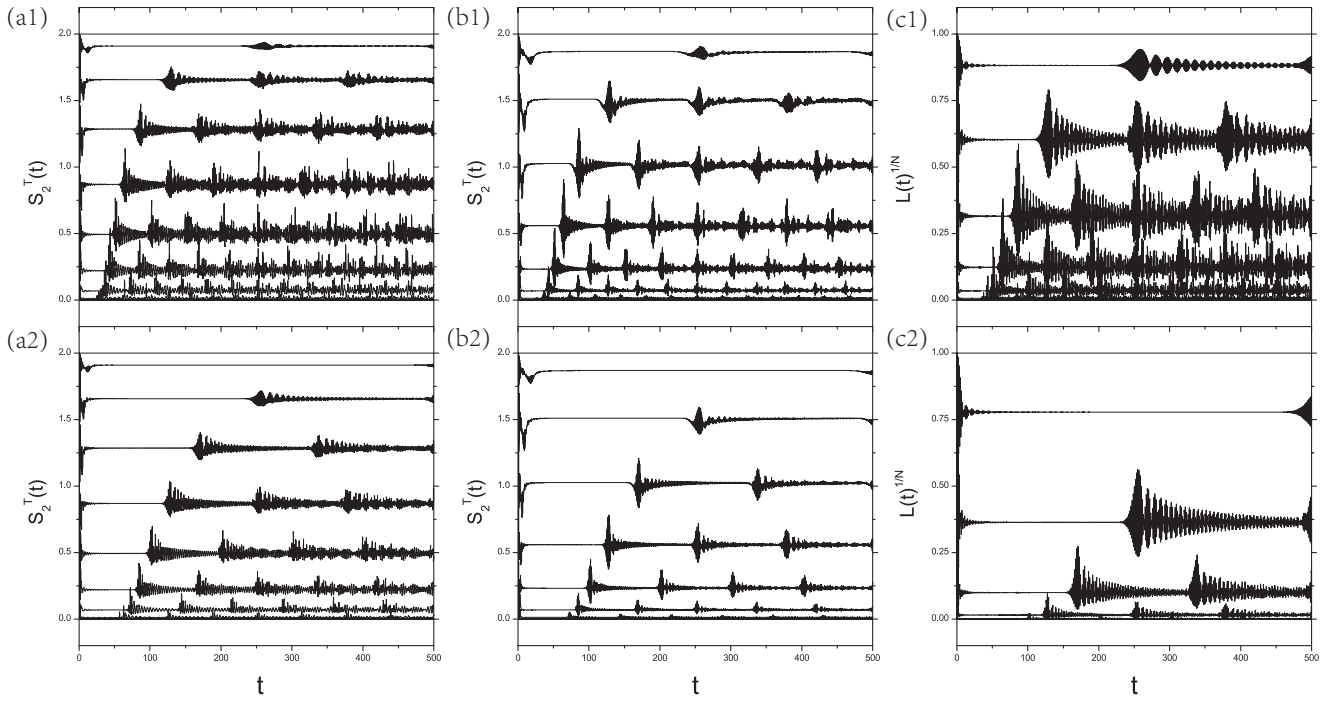

FIG. 5. Illustration of (a),(b) topological Rényi entropy and (c) Loschmidt echo after a quantum quench in finite time and with finite system size. In each plot, 16 distinct curves from top to bottom correspond to the different $\lambda = \lambda_x = \lambda_z$ from 0 to 1.5 in intervals of 0.1. The subsystem and system size are (a1) $R = 5$, $r = 1$, $N = 100$; (a2) $R = 5$, $r = 1$, $N = 200$; (b1) $R = 8$, $r = 2$, $N = 100$; (b2) $R = 8$, $r = 2$, $N = 200$; (c1) $N = 100$; and (c2) $N = 200$. We can see that the revival time of TE and LE is proportional to the system size N and is also dependent on λ, which means $t_* \sim N/v(\lambda)$. $v(\lambda)$ is the speed of signals in the system given by the Lieb-Robinson bounds as $v \sim \lambda$. The time average value of TE for each λ is equal to TE of the dephased state, which converges to the value for thermodynamic limit ($N \to \infty$) and $t \to \infty$ limit. We can also find that, as the size of the subsystem gets larger, TE is smaller with the same quench Hamiltonian $H(\lambda)$. After a quench, TE is almost completely destroyed when (a) $\lambda > 0.8$ and (b) $\lambda > 0.7$, which is compatible to the situation of $N \to \infty$ and $t \to \infty$.

observables of the system. It is then quite natural to foresee the same scenario for a nonintegrable quench, when there are not even local conserved quantities, and one would expect at large times to reach the Gibbs state locally.

As we mentioned above, it is important to address the question of the finite size for the subsystem. To this end, we show in Fig. 4(d), a one-dimensional cross section of the previous graph for clarity. We find that TE measured by S_2^T depends on subsystem size mostly through r_m, the size of the hole of subsystem (1). Indeed, keeping r_m constant and changing r only results in a variation of S_2^T of the order of 10^{-3} when $r_m \geqslant 5$. This fact is compatible with the thermal behavior of the TE in Ref. [59], where it was shown that, at finite temperature, TE is an explicit function of r_m^2 and temperature. We want to evaluate what is the minimum value of λ that destroys TE for a given size r_m. We define a thermalization point λ^* where $S_2^T(\lambda^*, t \to \infty) < \varepsilon$ and find that as subsystem size increases, λ^* becomes smaller. In the inset of Fig. 4(d), we plot the polynomial fit of function $\lambda^*(1/r_m)$ with fixed $r = 2$. Setting $\varepsilon = 10^{-3}$, we sample r_m as (5, 6, 7, 8, 9, 10, 11), and the corresponding λ^* is (0.69, 0.60, 0.53, 0.47, 0.42, 0.38, 0.35). The fit function is $\lambda^* = 4.22\frac{1}{r_m} - 3.76\frac{1}{r_m^2} + O(\frac{1}{r_m^3})$, which estimates the asymptotic behavior of λ^* getting closer to zero as r_m gets larger.

So far, we have presented the results for the limit of infinite time (and in the thermodynamic limit), as the correlation functions in Eq. (11) have a compact analytic form in the limit $t \to \infty$ (see the Appendix). However, we are interested also in understanding how fast thermalization is. We know that at infinite time, TE is completely destroyed (or halved with gauge symmetry) for the infinite subsystem, or it sets to a finite value for the finite subsystem if the quench parameter λ is not too large. We ask ourselves at what characteristic time t_{eq} this would happen. To this end, we just need to evaluate the time-dependent correlation functions in Eq. (11). The results are displayed in Fig. 5, where we show the time evolution of $S_2^T(t)$ for a subsystem of size (a) $R = 5$, $r = 1$ and (b) $R = 8$, $r = 2$ for different values of the quench strength $\lambda = \lambda_x = \lambda_z$. We can clearly see that after a very short time TE thermalizes. Moreover, TE acquires some revivals at later times, well before the recurrence time (that is double exponential in the system size; see Ref. [85]). One can already see that the time scale for thermalization depends on the size of the subsystem R,r, although we do not have enough points to make an estimate. However, the structure of the revivals for different system sizes and strengths of the quench λ is much clearer. Revivals are expected when the wave packet is partially reformed after signals in the system recombine [86,87]. As the speed v of signals in the system is given by the Lieb-Robinson bound as $v \sim \lambda$ [86–92], we can see that the time t_* at which the revival on the profile of $S_2^T(t)$ is reached scales like λ^{-1}. Revivals in the full wave function $|\Psi(t)\rangle$ are detected by the Loschmidt echo (LE), defined as $L_t := |\langle\Psi(t)|\Psi(0)\rangle|^2$ [93]. We show the behavior of LE in

panel (c) of Fig. 5. As one can see, TE and LE display the same time structure of revivals. Since L_t is very difficult to detect for an extended system, as it rapidly (exponentially) shrinks to zero with system size [93], it is actually desirable to find better observables to detect the structure of revivals. As we can see in Fig. 5, the topological Rényi entropy does detect the same revival times for a much larger set of system sizes, while the Loschmidt echo becomes featureless for stronger quenches in larger systems; see Fig. 5(c2) for the system with $N = 200$ spins. It is very interesting that one can use S_2^T as a probe of both the thermalization and the witness of the system still being away from equilibrium. Thermalization under unitary evolution is, in fact, thermalization in probability, meaning that the probability of observing a value different from the typical value goes to zero in the thermodynamic limit. We notice here that, in order to completely lose revivals in the TE, one also needs the thermodynamic limit of the subsystem. The same limits is also needed to get rid of the finite size effects in TE, as one can see in Fig. 4.

At this point, some more comments are in order regarding some other subtleties about the geometry of the subsystem. In the case where the subsystem is "thin," that is, consisting only of boundary, we find a residual topological entropy TE. However, the addition of a bulk makes it disappear (or reduce to its half value in case of gauge symmetry). In Ref. [62] it was demonstrated that, for the thin subsystem, the full value $S_2^T = 2$ was preserved. We find the same result with the formula presented here if we apply it to the thin subsystem, so the two results agree. Anyway, now we see that we have two ways of measuring S^T that yield two different results. If S^T is measured in a subsystem with bulk, we find thermal behavior, while, on the other hand, if the subsystem is thin, we find a more robust behavior. We are thus in a quandary: Which of the two ways is the right way to detect topological order? At zero temperature and for static perturbations the two ways give comparable results. Instead, these two subsystems give completely different results in the dynamical behavior. This is explained by the fact that TE defined as in Eq. (5) is equal to "quantum conditional mutual information" [94]; however, this is only true when the subsystem has a bulk. When we compute TE in the ground state, this is not crucial, because area law holds, so even in the thin subsystem case the boundary term of entanglement entropy is canceled out and therefore we can extract TE. On the other hand, in the case of quantum quench, high-energy eigenstates are involved and entanglement area law needs not to hold in general. However, "quantum conditional mutual information," i.e., TE for a subsystem with bulk, is still a good measurement of "long-range" correlation for a state without entanglement area law. As it was argued in Ref. [62], the topological entropy associated with a subsystem with bulk is associated with the existence of protected information in the system and with the confinement-deconfinement transition for the topological quasiparticles [95]. So we believe that this is the quantity of merit to detect topological order in a wave function.

IV. CONCLUSIONS AND OUTLOOK

In this paper, we presented a fully analytical treatment of the time evolution of the topological Rényi entropy S_2^T in the two-dimensional toric code after an integrable quantum quench. The main result of the paper is that S_2^T quickly reaches a thermal value. Therefore, even though the quench is integrable, the dynamics is complex enough to make the topological order thermalize. In two spatial dimensions, this amounts to destroying the topological order. In this work, dynamical and thermal stability of topological order are unified for the model under consideration. The technical result has been obtained by mapping the calculation of TE in the sum of many-point correlation functions. This result and the associated technique point to several directions for further study. First, we believe that the unification of dynamical and thermal features can be generalized. It is thus conceivable that if topological order survives a quantum quench, then it would be also thermally stable, and vice versa. This opens the way to studying thermal stability of other models that feature topological order, like the toric code in higher dimensions [25,26,96]. Moreover, the technique established here can be directly extended to the case of a quench with weak or strong disorder [97,98]. In one-dimensional spin chains, weak disorder may cause Anderson localization for free fermionic systems while strong disorder together with interactions may cause many-body localization (MBL) in the interacting case [97,99–102]. Very little is known about MBL in 2D and nothing about whether MBL is possible together with TO. In the presence of disorder, the system would be not fully integrable, but still amenable to analytical treatment, as we can still map the system to free fermions and then proceed numerically to diagonalize an $N \times N$ matrix [103,104] (as opposed to an exponentially large matrix). Moreover, one can use unitary perturbation theory [70] in combination with our technique. In this way, we can explore directly if there is many-body localization in presence of topological order [105,106] and if localization does protect it after a quantum quench or in temperature.

ACKNOWLEDGMENTS

This work was supported in part by the National Basic Research Program of China Grants No. 2011CBA00300 and No. 2011CBA00301 the National Natural Science Foundation of China Grants No. 61033001, No. 61361136003, No. 11574176 (A.H.), and No. 91536108 (H.F.).

APPENDIX

1. Mapping to Ising chains

The ground-state manifold $\mathscr{L}$ of the TCM is fourfold degenerate. Each ground state is the uniform superposition of closed strings. These closed strings can be arranged in four sectors according to contractible and noncontractible loops on the torus. The four-dimensional algebra $L(\mathscr{L})$ is generated by two pairs of topological operators (W_1^x, W_1^z) and (W_2^x, W_2^z). W_a^α is defined as

$$W_a^\alpha = \prod_{j \in \gamma_a^\alpha} \sigma_a^\alpha, \quad \alpha = x,z \quad a = 1,2. \tag{A1}$$

Each γ_a^α is a noncontractible curve along the toric on the lattice or the dual lattice (see Fig. 1). The external fields generate excitations described by open strings. Therefore, when the

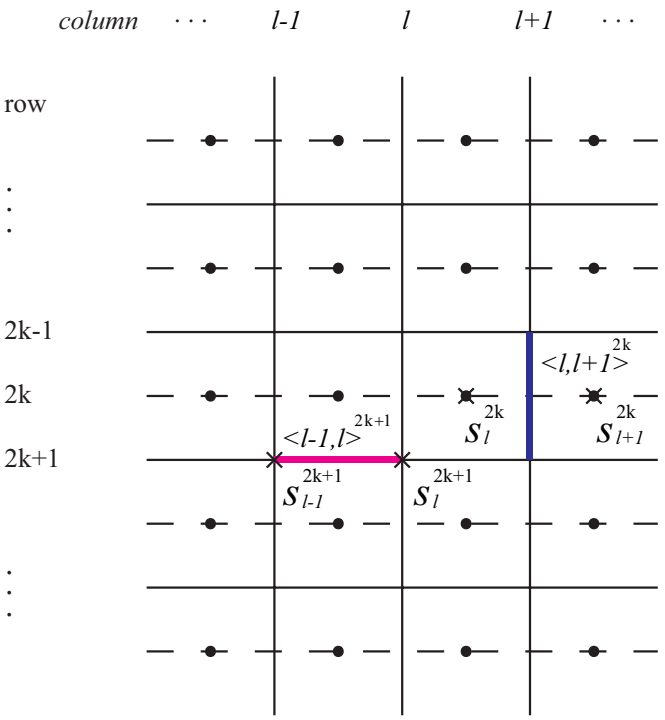

FIG. 6. Illustration of notations of sites (crosses) and links (red and blue bold segments) with row and column index. The physical spins live on the links (σ picture), while the effective spins live on the sites (τ picture). Site notation s_j^i with odd (even) row index belongs to lattice (dual lattice).

fields are turned on, the ground state is a superposition of both closed and open strings.

Because of the arrangement of the fields in horizontal and vertical lines, the Hamiltonian Eq. (8) can be reduced into two mutually commutative parts, $H = H_1 + H_2$, where

$$H_1 = -\sum_s A_s - \lambda_z \sum_{i\in h} \sigma_i^z,$$
$$H_2 = -\sum_p B_p - \lambda_x \sum_{i\in v} \sigma_i^x. \tag{A2}$$

As it is easy to verify, the two satisfy $[H_1, H_2] = 0$. For clarity, We use the symbol s_j^i to denote the site of the lattice or dual lattice at row i and column j, and symbol $\langle j, j+1\rangle^i$ to denote the bond located between s_j^i and s_{j+1}^i. Especially, when $i = 2k-1$ is odd, s_l^{2k-1} belongs to the lattice; when $i = 2k$ is even, s_l^{2k} belongs to the dual lattice (see Fig. 6). Noticing that $\{A_{s_l^{2k-1}}, \sigma^z_{\langle l,l+1\rangle^{2k-1}}\} = 0$ and $\{A_{s_{l+1}^{2k-1}}, \sigma^z_{\langle l,l+1\rangle^{2k-1}}\} = 0$, we can introduce the effective spins $\tau^z_{s_l^{2k-1}} \equiv A_{s_l^{2k-1}}$ and $\tau^x_{s_l^{2k-1}} \equiv \prod_{j\leqslant l} \sigma^z_{\langle j-1,j\rangle^{2k-1}}$ living on the lattice sites, so we have $\sigma^z_{\langle l,l+1\rangle^{2k-1}} = \tau^x_{s_l^{2k-1}} \tau^x_{s_{l+1}^{2k-1}}$. Then H_1 can be mapped to the effective spin form:

$$\tilde{H}_1 = -\sum_{k=1}^{N} \hat{K}_{2k-1} \equiv -\sum_{k=1}^{N} \left(\sum_{l=1}^{N} \tau^z_{s_l^{2k-1}} + \lambda_z \tau^x_{s_l^{2k-1}} \tau^x_{s_{l+1}^{2k-1}} \right). \tag{A3}$$

Similarly, H_2 can be mapped into $\tilde{H}_2$ by carrying out the procedure of $B_{s_l^{2k}} \equiv \tau^z_{s_l^{2k}}$ and $\sigma^x_{\langle l,l+1\rangle^{2k}} \equiv \tau^x_{s_l^{2k}} \tau^x_{s_{l+1}^{2k}}$, where the effective spins $\tau^z_{s_l^{2k}}$ and $\tau^x_{s_l^{2k}}$ live on the dual lattice sites. $\tilde{H}_2$ is written explicitly as

$$\tilde{H}_2 = -\sum_{k=1}^{N} \hat{K}_{2k} \equiv -\sum_{k=1}^{N} \left(\sum_{l=1}^{N} \tau^z_{s_l^{2k}} + \lambda_x \tau^x_{s_l^{2k}} \tau^x_{s_{l+1}^{2k}} \right). \tag{A4}$$

Adding $\tilde{H}_1$ and $\tilde{H}_2$ up, we finally get the Hamiltonian represented by the effective spins:

$$\tilde{H} = -\sum_{i=1}^{2N} \hat{K}_i \equiv -\sum_{i=1}^{2N} \left[\sum_{j=1}^{N} \tau^z_{s_j^i} + \lambda(i) \tau^x_{s_j^i} \tau^x_{s_{j+1}^i} \right],$$
$$\lambda(i) = \lambda_z, \quad i \text{ is odd},$$
$$\lambda(i) = \lambda_x, \quad i \text{ is even}. \tag{A5}$$

Equation (A5) shows that each term $\hat{K}_i$ is an Ising chain. Since the chains on different lines i are not coupled, namely $[\hat{K}_m, \hat{K}_n] = 0$, each Ising chain can be independently exactly solved by means of usual techniques involving Jordan-Wigner transformation, a Fourier transformation, and finally a Bogoliubov transformation [82,84]. Moreover, the eigenstate of Eq. (A5) has the tensor product form,

$$|\Psi\rangle = \otimes_{i=1}^{2N} |\Psi_i\rangle, \tag{A6}$$

in which $|\Psi_i\rangle$ is the eigenstate of the ith Ising chain. From now on, we call the representation in terms of the effective spin operators τ_s^z, τ_s^x the τ picture. The τ spins live on the sites of the lattice and the dual lattice, while the original σ picture represents the physical spins living on the bonds of the lattice (see Fig. 6). What we need to pay attention to is that there is one constraint in each Ising chain caused by periodic boundary condition. It corresponds to the constraints in σ picture:

$$\prod_{j=1}^{N} \sigma^z_{\langle j-1,j\rangle^{2k-1}} = 1,$$
$$\prod_{j=1}^{N} \sigma^x_{\langle j-1,j\rangle^{2k}} = 1, \quad k = 1,2,\ldots,N. \tag{A7}$$

Notice that the operators $w_k^z = \prod_{j=1}^{N} \sigma^z_{\langle j-1,j\rangle^{2k-1}}$ and $w_k^x = \prod_{j=1}^{N} \sigma^x_{\langle j-1,j\rangle^{2k}}$ are the topological operators in TCM, which means W_2^z and W_1^x. From now on, whenever the operator W_1^x (W_2^z) occurs, we mean that it is just an arbitrary w_k^x (w_k^z). They all commute with H, so we have $2N$ conserved quantities. If we denote the whole Hilbert space as $\mathscr{H}$ (σ picture) which dimension is 2^{2N^2}, we can choose the sector

$$\mathscr{H}' = \{|\Psi\rangle \in \mathscr{H} \mid w_k^z|\Psi\rangle = |\Psi\rangle, \quad w_k^x|\Psi\rangle = |\Psi\rangle,$$
$$k = 1,2,\ldots,N\}, \tag{A8}$$

whose dimension is 2^{2N^2-2N}. In this sector, both $\prod_{j=1}^{N} A_{s_j^{2k-1}}$ and $\prod_{j=1}^{N} B_{s_j^{2k}}$ equal to identity. We can write these constraints in the τ picture as

$$\prod_{j=1}^{N} \tau^z_{s_j^{2k-1}} = 1, \quad \prod_{j=1}^{N} \tau^z_{s_j^{2k}} = 1, \quad k = 1,2,\ldots,N. \tag{A9}$$

These constraints, together with the periodic boundary condition, give the corresponding sector $\mathscr{H}'$ in the τ picture.

2. Derivation of the formula for the purity

In this section, we find a general formula to compute the purity for a generic state in $\mathscr{H}'$ that is factorizable in the product on different lines i as in Eq. (A6). In this way, this formula can be used to compute the purity of every eigenstate of the Hamiltonian Eq. (8) or of the time evolution, including the one induced by a sudden quantum quench.

First, we need to choose a reference state which is a vector in $\mathscr{L}$ and also in $\mathscr{H}'$. As it is immediate to verify, the following state is a vector in $\mathscr{L}$:

$$|0'\rangle \equiv |G|^{-1/2} \sum_{g\in G} g|\Uparrow\rangle, \tag{A10}$$

where $|\Uparrow\rangle$ is the state with all spins pointing up in the z basis, namely $\sigma_i^z|\Uparrow\rangle = |\Uparrow\rangle$, $\forall\, i$. G is the group generated by the N^2-1 independent star operators A_s. The state Eq. (A10) is the simultaneous eigenstate of W_1^z and W_2^z with eigenvalue 1. However, it is not the the vector in the sector $\mathscr{H}'$. It is more convenient to choose, as reference state, the following state in $\mathscr{H}'$ (also in $\mathscr{L}$):

$$|0\rangle = \frac{1+W_1^x}{\sqrt{2}}|0'\rangle = (2|G|)^{-1/2} \sum_{g\in G} g\left(1+W_1^x\right)|\Uparrow\rangle. \tag{A11}$$

This state belongs to a different topological sector, which is the eigenstate of W_1^x and W_2^z with eigenvalue 1. Any state in $\mathscr{H}'$ can be written as

$$|\Psi\rangle = \sum_{x\in X}\sum_{z\in Z} b(xz)zx|0\rangle. \tag{A12}$$

The group $X(Z)$ has the tensor product form $X = \otimes_{k=1}^N X_k$ ($Z = \otimes_{k=1}^N Z_k$). One defines strings of x type as the strings running on the dual lattice and connecting the centers of plaquettes, and acting as $\hat{\sigma}^x$ on all the spins intersected by the string. Likewise, the strings of type z act like $\hat{\sigma}^z$ on all the spins traversed by strings running on the links of the lattice and connecting the sites of the lattice (see Fig. 1). The elements of each $X_k(Z_k)$ are the open strings of $x(z)$ type, mod $\{1, W_1^x\}$ ($\{1, W_2^z\}$), lying on the $2k$th [$(2k-1)$th] row. The number of open strings' end points is even, so the number of independent open strings is $[\sum_{m=1}^{[N/2]} \binom{N}{2m}]^{2N} = 2^{2N^2-2N}$, which conforms to the dimension of $\mathscr{H}'$.

As we noticed above, in the view of the τ picture, $|\Psi\rangle$ and $|0\rangle$ have tensor product form: $|\Psi_\tau\rangle = |\Psi_1\rangle\cdots|\Psi_{2N^2}\rangle$ and $|0_\tau\rangle = |0_1\rangle\cdots|0_{2N^2}\rangle$. Let us introduce the following notation for $|\psi\rangle$ and $|\phi\rangle$ as

$$|\Psi_\tau\rangle : \begin{cases} |\psi\rangle = |\Psi_1\rangle|\Psi_3\rangle\cdots|\Psi_{2N^2-1}\rangle, \\ |\phi\rangle = |\Psi_2\rangle|\Psi_4\rangle\cdots|\Psi_{2N^2}\rangle, \end{cases} \tag{A13}$$

and

$$|0_\tau\rangle : \begin{cases} |0_\psi\rangle = |0_1\rangle|0_3\rangle\cdots|0_{2N^2-1}\rangle, \\ |0_\phi\rangle = |0_2\rangle|0_4\rangle\cdots|0_{2N^2}\rangle. \end{cases} \tag{A14}$$

The following orthonormality conditions can be easily proven in the τ picture,

$$\begin{aligned}\langle 0|xz|0\rangle &= \langle 0_\psi|\tau(x)|0_\psi\rangle\langle 0_\phi|\tau(z)|0_\phi\rangle \\ &= \delta_{z,\mathbb{1}_Z}\delta_{x,\mathbb{1}_X}, \quad \forall\, x\in X, \quad \forall\, z\in Z,\end{aligned} \tag{A15}$$

and

$$b(xz) = \langle 0|xz|\Psi\rangle = \langle 0_\psi|\tau(x)|\psi\rangle\langle 0_\phi|\tau(z)|\phi\rangle \equiv b(x)b(z), \tag{A16}$$

where $\tau(x)$ [$\tau(z)$] is the operator mapped from the σ picture to the τ picture. Combining Eqs. (A10), (A11), and (A12), we get

$$|\Psi\rangle = (2|G|)^{-1/2} \sum_{x\in X}\sum_{g\in G}\sum_{z\in Z} b(xz)zxg\left(1+W_1^x\right)|\Uparrow\rangle. \tag{A17}$$

Now we introduce a new group Y for the convenience of the later derivation, which is defined as

$$Y = X\times G\times\left\{1, W_1^x\right\}. \tag{A18}$$

The generators of Y are constituted by all the generators of X, G, and W_1^x apparently, but we can also give a different description that will become useful later. As one can easily verify, the group can be generated by two types of operators which live on either even lines or odd lines. (1) The generators on the $(2k)$th line are $\sigma^x_{\langle i,i+1\rangle^{2k}}$, with $i = 1,2,\ldots,N$. (2) The generators on the $(2k-1)$th line are $\sigma^x_{\langle i,i+1\rangle^{2k-1}}\sigma^x_{\langle i+1,i+2\rangle^{2k-1}}$, with $i = 1,2,\ldots,N-1$. Notice that the periodic boundary condition is applied. Thus, the order of Y is 2^{2N^2-N}, which is, of course, identical to $|X|\times|G|\times|\{1,W_1^x\}| = 2^{2N^2-N}$. So for any $x\in X$ and $g\in G\times\{1,W_1^x\}$ we have the following relationships:

$$\begin{aligned}&\forall\, x,g \quad \exists\, y\in Y, \quad \text{such that} \quad y = xg, \\ &b(xz) = b(gxz) = b(yz),\end{aligned} \tag{A19}$$

where we used Eq. (A16) and the fact that $g|0\rangle = |0\rangle$. By combining Eqs. (A18) and (A19), we rewrite Eq. (A17) as

$$|\Psi\rangle = (2|G|)^{-1/2} \sum_{z\in Z}\sum_{y\in Y} b(yz)zy|\Uparrow\rangle. \tag{A20}$$

Note that whether the operators z and y commute or not depends on the common links they shared. If they share even (odd) links, they commute (do not commute). The parity of the shared links number is denoted as $z\cap y$, namely,

$$zy = yz(-1)^{z\cap y}. \tag{A21}$$

Together with the fact that $z|\Uparrow\rangle = |\Uparrow\rangle$, Eq. (A20) turns out to be

$$|\Psi\rangle = (2|G|)^{-1/2} \sum_{z\in Z}\sum_{y\in Y}(-1)^{y\cap z} b(yz)y|\Uparrow\rangle. \tag{A22}$$

Now let us write the corresponding density operator. It reads

$$\begin{aligned}\rho = (2|G|)^{-1} &\sum_{z,z'\in Z}\sum_{y,y'\in Y} \bar{b}(z'y')b(yz) \\ &\times(-1)^{y\cap z+y'\cap z'}|y_A y_B\rangle\langle y'_A y'_B|,\end{aligned} \tag{A23}$$

where we have adopted the notation $y|\Uparrow\rangle = y_A|\Uparrow_A\rangle \otimes y_B|\Uparrow_B\rangle = |y_A y_B\rangle$. The reduced density operator to subsystem A is obtained by tracing over the B part:

$$\rho_A = (2|G|)^{-1} \sum_{z,z'\in Z} \sum_{y,y'\in Y} \bar{b}(z'y')b(yz) \times (-1)^{y\cap z + y'\cap z'} |y_A\rangle\langle y'_A| \langle y_B y'_B\rangle. \quad \text{(A24)}$$

Since we are summing over all the elements of the group, we can relabel the elements in the sum as $y' = y\tilde{y}$ to rewrite Eq. (A24) as

$$\rho_A = (2|G|)^{-1} \sum_{z,z'\in Z} \sum_{y,\tilde{y}\in Y} \bar{b}(z'y\tilde{y})b(yz) \times (-1)^{y\cap z + y\tilde{y}\cap z'} |y_A\rangle\langle y_A\tilde{y}_A|\langle\tilde{y}_B\rangle. \quad \text{(A25)}$$

Note that $\langle\tilde{y}_B\rangle$ is nonzero only when $\tilde{y}_B = \mathbb{1}_B$. We now introduce the subgroups $Y_A \in Y$ and $Y_B \in Y$:

$$Y_A \equiv \{y \in Y | y = y_A \otimes \mathbb{1}_B\}, \quad \text{(A26)}$$

$$Y_B \equiv \{y \in Y | y = \mathbb{1}_A \otimes y_B\}. \quad \text{(A27)}$$

Finally we get the reduced operator in form of

$$\rho_A = (2|G|)^{-1} \sum_{z,z'\in Z} \sum_{\substack{y\in Y \\ \tilde{y}\in Y_A}} \bar{b}(z'y\tilde{y})b(yz) \times (-1)^{y\cap z + y\tilde{y}\cap z'} |y_A\rangle\langle y_A\tilde{y}_A|. \quad \text{(A28)}$$

Let us now make a remark about the topological sector used in this derivation. The state $|\Psi\rangle$ we are interested in is a state away from equilibrium after quantum quench; that is, $|\Psi\rangle = e^{-iH(\lambda)t}|\Psi(0)\rangle$. The initial state $|\Psi(0)\rangle$ is a ground state of toric code Hamiltonian $H(\lambda = 0)$, which we prepared at $t = 0$. In the derivation, the state $|\Psi(0)\rangle$ (also $|\Psi\rangle$) is constrained to the sector $\mathscr{H}'$, which is the eigenspace of $W_1^x = 1$ and $W_2^z = 1$, that is $|\Psi(0)\rangle = |0\rangle$. However, topological entropy is not affected by this restriction. Following Ref. [13], we can show that the reduced density matrix $\rho_A = \mathrm{Tr}_B[|\Psi\rangle\langle\Psi|]$ is independent on the topological sector, and thus there is no loss of generality in fixing it. Indeed, by denoting the following four states $|\xi_{ij}\rangle, i, j = 0, 1$ as a basis in the ground-state manifold $\mathscr{L}$,

$$|\xi_{ij}\rangle = \left(W_1^z\right)^i \left(W_2^x\right)^j |0\rangle, \quad \text{(A29)}$$

we see that they satisfy $W_1^x|\xi_{ij}\rangle = (-1)^i|\xi_{ij}\rangle$ and $W_2^z|\xi_{ij}\rangle = (-1)^j|\xi_{ij}\rangle$. An arbitrary state in $\mathscr{L}$ can be written as

$$|\tilde{\xi}\rangle = \sum_{i,j=0}^{1} \alpha_{ij}|\xi_{ij}\rangle, \quad \text{(A30)}$$

where $\sum_{i,j=0}^{1} |\alpha_{ij}|^2 = 1$. After the same procedure showed in Eq. (A12), we can get the corresponding $|\tilde{\Psi}_{ij}\rangle$ and also $|\tilde{\Psi}\rangle$ as

$$|\Psi_{ij}\rangle = \sum_{x\in X} \sum_{z\in Z} b(xz)zx|\xi_{ij}\rangle \quad \text{(A31)}$$

and

$$|\tilde{\Psi}\rangle = \sum_{i,j=0}^{1} \alpha_{ij}|\Psi_{ij}\rangle, \quad \text{(A32)}$$

where $W_1^x|\Psi_{ij}\rangle = (-1)^i|\Psi_{ij}\rangle$ and $W_2^z|\Psi_{ij}\rangle = (-1)^j|\Psi_{ij}\rangle$. The reduced density matrix of $|\tilde{\Psi}\rangle$ is

$$\tilde{\rho}_A = \sum_{i,j,k,l=0}^{1} \alpha_{ij}\alpha_{kl}^* \mathrm{Tr}_B[|\Psi_{ij}\rangle\langle\Psi_{kl}|]. \quad \text{(A33)}$$

We can thus prove that $\mathrm{Tr}_B[|\Psi_{ij}\rangle\langle\Psi_{kl}|] = \delta_{ij,kl}\mathrm{Tr}_B[|\Psi_{00}\rangle\langle\Psi_{00}|] = \rho_A$. A similar proof was showed in Ref. [13], where the fact that contractible loops cannot generate noncontractible loop was used. Noticing that contractible loops and independent open strings also cannot generate noncontractible loops, the proof can be directly generalized. We therefore have

$$\tilde{\rho}_A = \rho_A. \quad \text{(A34)}$$

$|\tilde{\Psi}\rangle$ belongs to the space $\tilde{\mathscr{H}}$, which is defined as

$$\tilde{\mathscr{H}} = \left\{ |\Psi\rangle \in \mathscr{H} \mid \prod_{j=1}^{N} A_{s_j^{2k-1}}|\Psi\rangle = |\Psi\rangle, \prod_{j=1}^{N} B_{s_j^{2k}}|\Psi\rangle = |\Psi\rangle, k = 1,2,\ldots,N \right\}. \quad \text{(A35)}$$

Paying attention to the global constraint of $\prod_s A_s = 1$ and $\prod_p B_p = 1$, we have $\dim(\tilde{\mathscr{H}}) = 4\dim(\mathscr{H}')$. Also we have $\mathscr{H}' \subset \tilde{\mathscr{H}}$ and $\mathscr{L} \subset \tilde{\mathscr{H}}$ (note that $\mathscr{L} \not\subset \mathscr{H}'$).

Now we move on to the calculation of the purity of ρ_A, which is $P = \mathrm{Tr}[\rho_A^2]$, following directly as

$$P = (2|G|)^{-2} \sum_{\substack{z_1,z_2\in Z \\ z'_1,z'_2\in Z}} \sum_{\substack{y_1,y_2\in Y \\ \tilde{y}_1,\tilde{y}_2\in Y_A}} \bar{b}(z'_1 y_1 \tilde{y}_1) \times b(y_1 z_1)\bar{b}(z'_2 y_2 \tilde{y}_2)b(y_2 z_2) \times (-1)^{y_1\cap z_1 + y_1\tilde{y}_1\cap z'_1 + y_2\cap z_2 + y_2\tilde{y}_2\cap z'_2} \times \langle y_{1A}\tilde{y}_{1A}y_{2A}\rangle\langle y_{2A}\tilde{y}_{2A}y_{1A}\rangle. \quad \text{(A36)}$$

Note that the term $\langle y_{1A}\tilde{y}_{1A}y_{2A}\rangle\langle y_{2A}\tilde{y}_{2A}y_{1A}\rangle$ imposes two constrains, (1) $\tilde{y}_1 = \tilde{y}_2$ and (2) $y_2 = y_1\tilde{y}_1\bar{y}$, where $\bar{y} \in Y_B$. Thus, the purity formula can be simplified as

$$P = (2|G|)^{-2} \sum_{\substack{z_1,z_2\in Z \\ z'_1,z'_2\in Z}} \sum_{\substack{y\in Y \\ \tilde{y}\in Y_A \\ \bar{y}\in Y_B}} \bar{b}(z'_1 y\tilde{y})b(yz_1)\bar{b}(z'_2 y\bar{y})b(y\tilde{y}\bar{y}z_2) \times (-1)^{y\cap z_1 + y\tilde{y}\cap z'_1 + y\tilde{y}\bar{y}\cap z_2 + y\bar{y}\cap z'_2}. \quad \text{(A37)}$$

For further simplification, we rewrite the last term as

$$(-1)^{y\cap z_1 + y\tilde{y}\cap z'_1 + y\tilde{y}\bar{y}\cap z_2 + y\bar{y}\cap z'_2} = (-1)^{\tilde{y}\cap z'_1 + \tilde{y}\cap z_2}(-1)^{y\cap z_1 z'_1 z_2 z'_2}(-1)^{\bar{y}\cap z_2 z'_2}. \quad \text{(A38)}$$

The above equality can be easily proven by the fact that

$$y_1\cdots y_k z_1\cdots z_l = z_1\cdots z_l y_1\cdots y_k(-1)^{g_1\cdots g_k\cap z_1\cdots z_l},$$
$$y_1\cdots y_k z_1\cdots z_l = z_1\cdots z_l y_1\cdots y_k \prod_{i=1}^{k}\prod_{j=1}^{l}(-1)^{y_i\cap z_j}. \quad \text{(A39)}$$

The first equation is deduced as we commute the $(y_1\cdots y_k)$ and $(z_1\cdots z_l)$ as two operators while in the second equation

we commute each y_i and z_j at a time. Now, recalling that $\bar{b}(z_1' y\tilde{y}) b(y\tilde{y}\bar{y}z_2)$ is equal to $\langle\Psi|z_1' y\tilde{y}|0\rangle\langle 0|y\tilde{y}\bar{y}z_2|\Psi\rangle$, we have

$$\begin{aligned}
&\bar{b}(z_1' y\tilde{y}) b(y\tilde{y}\bar{y}z_2)(-1)^{\tilde{y}\cap z_1' + \tilde{y}\cap z_2} \\
&\quad = \langle\Psi|z_1' y\tilde{y}|0\rangle\langle 0|y\tilde{y}\bar{y}z_2|\Psi\rangle(-1)^{\tilde{y}\cap z_1' + \tilde{y}\cap z_2} \\
&\quad = \langle\Psi|\tilde{y}z_1' y|0\rangle\langle 0|y\bar{y}z_2\tilde{y}|\Psi\rangle, \qquad \text{(A40)}
\end{aligned}$$

where we have employed that every two elements in group Y commute. Combining this equation, Eq. (A37) is simplified to be

$$\begin{aligned}
P = (2|G|)^{-2} \sum_{\substack{z_1,z_2\in Z \\ z_1',z_2'\in Z}} \sum_{\substack{y\in Y \\ \tilde{y}\in Y_A \\ \bar{y}\in Y_B}} &\langle\Psi|\tilde{y}z_1' y|0\rangle\langle 0|yz_1|\Psi\rangle \\
&\times \langle\Psi|z_2' y\bar{y}|0\rangle\langle 0|y\bar{y}z_2\tilde{y}|\Psi\rangle \\
&\times (-1)^{y\cap z_1 z_1' z_2 z_2'}(-1)^{\bar{y}\cap z_2 z_2'}. \qquad \text{(A41)}
\end{aligned}$$

Notice that the above formula is written in the σ picture. In the following section, we obtain the exact state $|\Psi\rangle$ in the τ picture. Therefore, in order to proceed to further calculation, we first need to map this formula from the σ picture to the τ picture. We know how to map the group Z to the τ picture as we discussed earlier, but how about the group Y? One has to remember that Y is generated by two types of operators. Again, the first type of operators are generated by $\sigma^x_{\langle i,i+1\rangle^{2k}}$, with $i = 1,2,\ldots,N$ and $k = 1,2,\ldots,N$. These operators form a group X', which is homomorphic to the group X. Notice that both X and X' are constituted by tensor products of even lines, and the homomorphic mapping from X' to X in each row is 2 to 1 since X is a group containing only open strings while X' contains open strings and a noncontractible closed string in each line. In $\mathscr{H}'$, this noncontractible closed string acts as the identity operator. The homomorphic mapping from X' to X is 2^N to 1 since the number of even lines is N. So the order of X' is $|X'| = 2^{N^2}$ while $|X| = 2^{N^2-N}$. Clearly X' can be mapped to the τ picture. The second type is the operators generated by $\sigma^x_{\langle i,i+1\rangle^{2k-1}}\sigma^x_{\langle i+1,i+2\rangle^{2k-1}}$, with $i = 1,2,\ldots,N-1$ and $k = 1,2,\ldots,N$. In order to map them to the τ picture, we relabel them by the operators which belong to the group G and form the group $G' = Y/X'$. Precisely, $G' = G \times \{1, W_1^x\}/\prod_{k=1}^N \{1, w_k^x\}$. The description in the τ picture is more clear: G' has the tensor product form $G' = \otimes_{k=1}^N G_k'$ and each G_k' is generated by 2^{N-1} independent $\tau^z_{s_j^{2k-1}}$ with constraint $\prod_{j=1}^N \tau^z_{s_j^{2k-1}} = 1$ in the $(2k-1)$th row. Or we can say that G' is generated by the open strings of τ^z operators lying on the odd lines. So $|G'| = 2^{N^2-N}$ and $|Y| = |G'||X'| = 2^{2N^2-N}$, which coincide with the former discussion. Finally, the group Y can be written as

$$Y = G' \times X'. \qquad \text{(A42)}$$

The next step is to rewrite Y_A and Y_B. This part is a little difficult because of the constraints on the boundaries of subsystems A and B, which are shown in Fig. 7. One can verify that the relationships shown in Table I hold. In this table, the groups G', G_A', G_B', $\partial G_A'$, and $\partial G_B'$ are all subgroups of G. $\tilde{x}(\partial\tilde{g})$ and $\partial\bar{x}(\partial\bar{g})$ are the functions of $\partial\tilde{g}$ and $\partial\bar{g}$, respectively. Moreover, $G_A'(\subset G')$ is generated by all the independent star operators that act solely on subsystem A, while $G_B'(\subset G')$ is generated by all the independent star operators that act solely on subsystem B. The generators of $\partial G_A'$ and $\partial G_B'$ are shown in Fig. 7. They depend upon the shape of the subsystem A and we choose subsystem (2) to illustrate and one can get them for subsystems (1), (3), and (4).

Now we can map the spin operators in formula of purity Eq. (A41) to the τ picture. From now on, we do not distinguish the notations of all the groups concerned in the two pictures. The purity written in the τ picture finally reads:

$$P = \sum_{\substack{\partial\tilde{g}\in\partial G_A' \\ \partial\bar{g}\in\partial G_B'}} P_1(\partial\tilde{g},\partial\bar{g}) P_2(\partial\tilde{g},\partial\bar{g}), \qquad \text{(A43)}$$

where, recalling $|\psi\rangle$ and $|\phi\rangle$ defined in Eq. (A13), we have

$$\begin{aligned}
P_1(\partial\tilde{g},\partial\bar{g}) = \sum_{\substack{z_1,z_2\in Z \\ z_1',z_2'\in Z}} \sum_{\substack{g\in G' \\ \tilde{g}\in G_A' \\ \bar{g}\in G_B'}} &(2|G|)^{-2}\langle\psi|\tilde{g}\partial\tilde{g}z_1' g|0_\psi\rangle\langle 0_\psi|gz_1|\psi\rangle \\
&\times \langle\psi|z_2' g\bar{g}\partial\bar{g}|0_\psi\rangle\langle 0_\psi|g\bar{g}\partial\bar{g}z_2\tilde{g}\partial\tilde{g}|\psi\rangle \\
&\times (-1)^{g\cap z_1 z_1' z_2 z_2'}(-1)^{\bar{g}\cap z_2 z_2'}(-1)^{\partial\bar{g}\cap z_2 z_2'} \qquad \text{(A44)}
\end{aligned}$$

and

$$\begin{aligned}
P_2(\partial\tilde{g},\partial\bar{g}) = \sum_{\substack{x\in X' \\ \tilde{x}\in X_A' \\ \bar{x}\in X_B'}} &\langle\phi|\tilde{x}\partial\tilde{x}(\partial\tilde{g})x|0_\phi\rangle\langle 0_\phi|x|\phi\rangle\langle\phi|x\bar{x}\partial\bar{x}(\partial\bar{g})|0_\phi\rangle \\
&\times \langle 0_\phi|x\bar{x}\partial\bar{x}(\partial\bar{g})\tilde{x}\partial\tilde{x}(\partial\tilde{g})|\phi\rangle. \qquad \text{(A45)}
\end{aligned}$$

There are two points to notice. (i) The phase term does not appear in P_2 because of the fact that x and z live in even and odd rows, respectively, so they always commute. (ii) The notation $g \cap z$ in P_1 means the parity of the number of common sites shared by g and z in the τ picture. Remember that $g \cap z$ is the parity of common links in the σ picture as we have introduced before. The above expression can be simplified. Let us start with P_1. First, notice the fact that for any $g \in G$, we have $g|0_\psi\rangle = |0_\psi\rangle$, so the g type of operators in Eq. (A44) are absorbed by $|0_\psi\rangle$:

$$\begin{aligned}
&\langle\psi|\tilde{g}\partial\tilde{g}z_1' g|0_\psi\rangle\langle 0_\psi|gz_1|\psi\rangle\langle\psi|z_2' g\bar{g}\partial\bar{g}|0_\psi\rangle \\
&\quad\times\langle 0_\psi|g\bar{g}\partial\bar{g}z_2\tilde{g}\partial\tilde{g}|\psi\rangle \\
&= \langle\psi|\tilde{g}\partial\tilde{g}z_1'|0_\psi\rangle\langle 0_\psi|z_1|\psi\rangle\langle\psi|z_2'|0_\psi\rangle\langle 0_\psi|z_2\tilde{g}\partial\tilde{g}|\psi\rangle. \qquad \text{(A46)}
\end{aligned}$$

Next we work on the last phase term in Eq. (A44). We can prove the equation

$$\sum_{g\in G_R'}(-1)^{g\cap z} = \begin{cases} |G_R'| & z \in Z_{\bar{R}}, \\ 0 & z \notin Z_{\bar{R}}, \end{cases} \qquad \text{(A47)}$$

where $Z_{\bar{R}}$ is defined as $Z_{\bar{R}} \equiv \{z \in Z | \forall\, g \in G_R, zg = gz\}$. The proof goes as follows. If $\exists\, a \in G_R'$, such that $az = -za$, define quotient group $G_a \equiv G_R'/\{1,a\}$; thus, $G_R' = \{G_a, aG_a\}$. Then $\sum_{g\in G_R'}(-1)^{g\cap z} = \sum_{g\in G_a}(-1)^{g\cap z} + \sum_{g\in aG_a}(-1)^{g\cap z}$. The second term is equal to $\sum_{g\in G_a}(-1)^{ag\cap z} = \sum_{g\in G_a}(-1)^{g\cap z}(-1)^{a\cap z} = -\sum_{g\in G_a}(-1)^{g\cap z}$, since $az = -za$. So $\sum_{g\in G_R'}(-1)^{g\cap z} = 0$. If $\forall\, g \in G_R'$ satisfies $gz = zg, (-1)^{g\cap z} = 1$, so $\sum_{g\in G_R'}(-1)^{g\cap z} = \sum_{g\in G_R'} 1 = |G_R'|$. Combining Eqs. (A46)

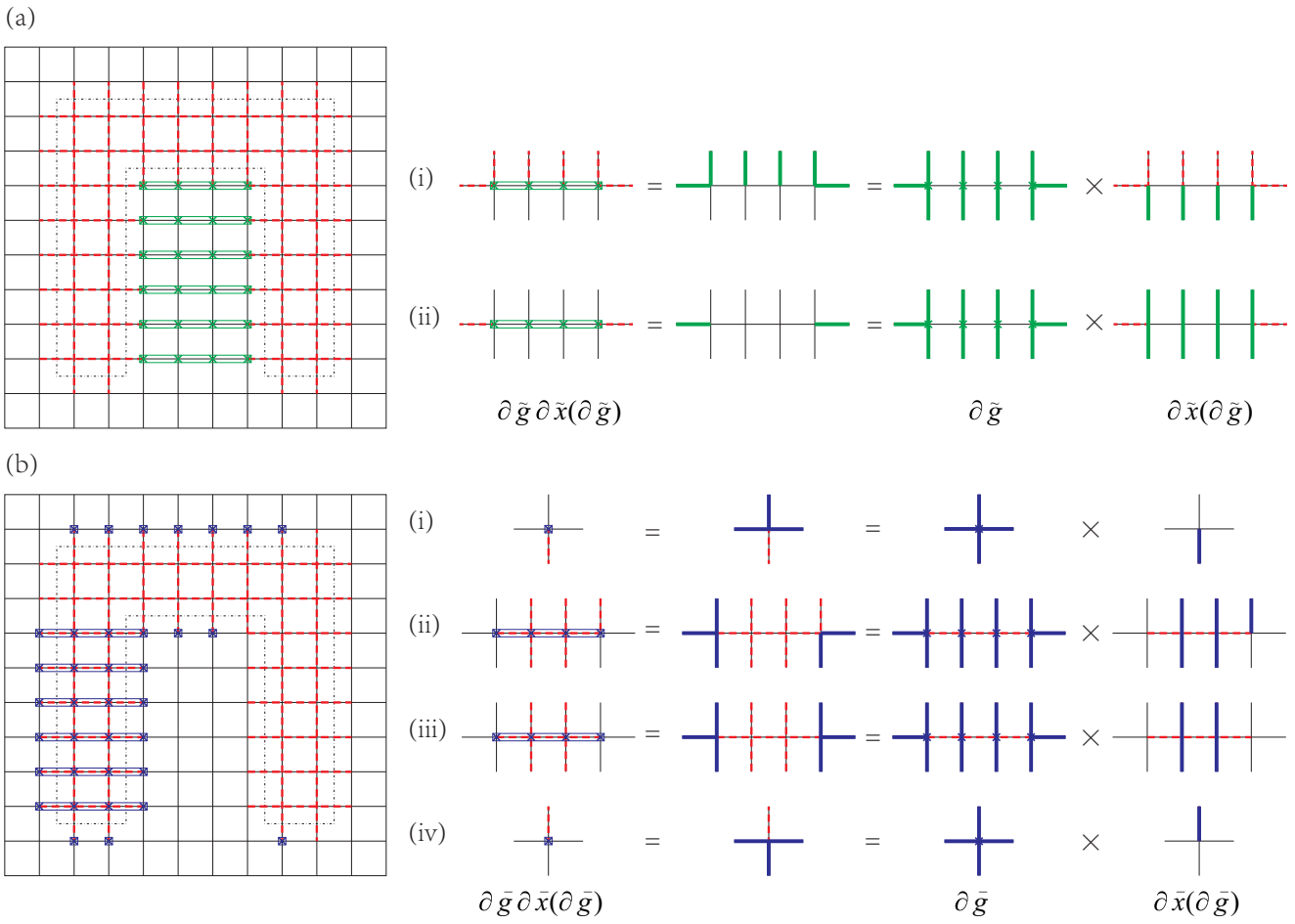

FIG. 7. Illustration of (a) $\partial\tilde{g}\partial\tilde{x}(\partial\tilde{g})$ operators that $\partial\tilde{g}\in\partial G'_A$ and (b) $\partial\bar{g}\partial\bar{x}(\partial\bar{g})$ operators that $\partial\bar{g}\in\partial G'_B$ in subsystem (2) with $R=8$, $r=2$. These collective operators are denoted as the (a) green crosses with rectangle blocks and (b) blue crosses with square or rectangle blocks. The (a) green and (b) blue solid lines on the right side are σ^x operators on the edges. (a) Each generator of $\partial G'_A$ is the product of star operators on the cross marked sites in each rectangle block. $\partial\tilde{x}$ is the function of $\partial\tilde{g}$ so that $\partial\tilde{g}\partial\tilde{x}(\partial\tilde{g})$ acts solely on A. There are two types of $\partial\tilde{g}\partial\tilde{x}(\partial\tilde{g})$ operators in subsystem (2). (b) The generators of $\partial G'_B$ are (i),(iv) the star operator on the cross marked site in each square block and (ii),(iii) the product of star operators on the cross marked sites in each rectangle block. $\partial\bar{x}$ is the function of $\partial\bar{g}$ so that $\partial\bar{g}\partial\bar{x}(\partial\bar{g})$ acts solely on B. There are four types of $\partial\bar{g}\partial\bar{x}(\partial\bar{g})$ operators in subsystem (2).

and (A47) and Eq. (A44), we get the relations $z_1z_1'z_2z_2'=1$ and $z_2z_2'=\tilde{z}\in Z_{\bar{B}}$. We prefer to rename the group $Z_{\bar{B}}$ as Z_A; thus, Eq. (A44) is simplified as

$$P_1(\partial\tilde{g},\partial\bar{g})=\frac{|G'||G'_B|}{(2|G|)^2}\sum_{\substack{z_1,z_2\in Z\\ \tilde{z}\in Z_A}}\sum_{\tilde{g}\in G'_A}\langle\psi|\tilde{g}\partial\tilde{g}\tilde{z}z_1|0_\psi\rangle\langle 0_\psi|z_1|\psi\rangle \times\langle\psi|\tilde{z}z_2|0_\psi\rangle\langle 0_\psi|z_2\tilde{g}\partial\tilde{g}|\psi\rangle(-1)^{\partial\tilde{g}\cap\tilde{z}}. \quad \text{(A48)}$$

Noticing the fact that $\sum_{z\in Z}z|0_\psi\rangle\langle 0_\psi|z=1$ and $2|G|=2^N|G'|$, we finally get

$$P_1(\partial\tilde{g},\partial\bar{g})=\frac{|G'_B|}{2^{2N}|G'|}\sum_{\tilde{z}\in Z_A}\sum_{\tilde{g}\in G'_A}|\langle\psi|\tilde{g}\partial\tilde{g}\tilde{z}|\psi\rangle|^2(-1)^{\partial\tilde{g}\cap\tilde{z}}. \quad \text{(A49)}$$

Now let us take care of P_2. Just like the group G' defined in odd rows, we define the corresponding group in even rows as H'. In the τ picture, H' has the tensor product form $H'=\otimes_{k=1}^N H'_k$ and each H'_k is generated by 2^{N-1} independent $\tau^z_{s_j^{2k}}$ constrained by $\prod_{j=1}^N\tau^z_{s_j^{2k}}=1$ in the $(2k)$th row. Now we rewrite $|0_\phi\rangle$ as

$$|0_\phi\rangle=|H'|^{-1/2}\sum_{h\in H'}h|\tilde{0}\rangle, \quad \text{(A50)}$$

where $|\tilde{0}\rangle$ has the tensor product form $|\tilde{0}\rangle\equiv|\tilde{0}_\phi\rangle=\otimes_{k=1}^N|\tilde{0}_{2k}\rangle$. It satisfies $x|\tilde{0}\rangle=|\tilde{0}\rangle$ for all $x\in X$ (it holds for $x\in X'$) and $\prod_{j=1}^N\tau^z_{s_j^{2k}}|\tilde{0}_{2k}\rangle=|\tilde{0}_{2k}\rangle$ for any k. Substitute the equation into

TABLE I. Decompositions of Group Y, Y_A, and Y_B.

$\forall\, y\in Y$	$\exists\, g\in G', x\in X'$	such that $y=gx$
$\forall\,\tilde{y}\in Y_A$	$\exists\,\tilde{g}\in G'_A,\partial\tilde{g}\in\partial G'_A,\tilde{x}\in X'_A$	such that $\tilde{y}=\tilde{g}\tilde{x}\partial\tilde{g}\partial\tilde{x}(\partial\tilde{g})$
$\forall\,\bar{y}\in Y_B$	$\exists\,\bar{g}\in G'_B,\partial\bar{g}\in\partial G'_B,\bar{x}\in X'_B$	such that $\bar{y}=\bar{g}\bar{x}\partial\bar{g}\partial\bar{x}(\partial\bar{g})$

Eq. (A45):

$$P_2 = |H'|^{-2} \sum_{\substack{h_1,h_2\in H' \\ h_1',h_1'\in H'}} \sum_{\substack{x\in X' \\ \tilde{x}\in X'_A \\ \bar{x}\in X'_B}} \langle\phi|\bar{x}\partial\bar{x}xh_1|\tilde{0}\rangle\langle\tilde{0}|h_1'x|\phi\rangle \times \langle\phi|x\bar{x}\partial\bar{x}h_2|\tilde{0}\rangle\langle\tilde{0}|h_2'x\bar{x}\partial\bar{x}\tilde{x}\partial\tilde{x}|\phi\rangle. \quad \text{(A51)}$$

By commuting some terms we obtain

$$P_2 = |H'|^{-2} \sum_{\substack{h_1,h_2\in H' \\ h_1',h_1'\in H'}} \sum_{\substack{x\in X' \\ \tilde{x}\in X'_A \\ \bar{x}\in X'_B}} \langle\phi|\bar{x}\partial\bar{x}h_1|\tilde{0}\rangle\langle\tilde{0}|h_1'|\phi\rangle \times \langle\phi|h_2|\tilde{0}\rangle\langle\tilde{0}|h_2'\tilde{x}\partial\tilde{x}|\phi\rangle \times (-1)^{x\cap h_1h_1'h_2h_2'}(-1)^{\bar{x}\cap h_2h_2'}(-1)^{\partial\bar{x}\cap h_2h_2'}. \quad \text{(A52)}$$

The story here is just like the P_1 part. Repeating the derivation we get

$$P_2(\partial\tilde{g},\partial\bar{g}) = \frac{2^{2N}|X'_B|}{|X'|} \sum_{\tilde{h}\in H'_A} \sum_{\tilde{x}\in X'_A} |\langle\phi|\bar{x}\partial\bar{x}(\partial\bar{g})\tilde{h}|\phi\rangle|^2 \times (-1)^{\partial\bar{x}(\partial\bar{g})\cap\tilde{h}}. \quad \text{(A53)}$$

The 2^{2N} term comes form $|X'| = 2^N|H'|$. Combing Eqs. (A49) and (A53), we finally get the purity formula,

$$P = C_P \sum_{\partial\bar{g}\in\partial G'_A} \sum_{\substack{\tilde{g}\in G'_A \\ \tilde{z}\in Z_A}} |\langle\psi|\tilde{g}\partial\tilde{g}\tilde{z}|\psi\rangle|^2 \sum_{\substack{\tilde{h}\in H'_A \\ \tilde{x}\in X'_A}} |\langle\phi|\tilde{x}\partial\tilde{x}(\partial\tilde{g})\tilde{h}|\phi\rangle|^2 \times \sum_{\partial\bar{g}\in\partial G'_B} (-1)^{\partial\bar{g}\partial\bar{x}(\partial\bar{g})\cap\tilde{z}\tilde{h}}, \quad \text{(A54)}$$

where the coefficient $C_P = \frac{|G'_B|}{|G'|}\frac{|X'_B|}{|X'|}$ can be presented as $2^{R+2}2^{-(\#A+\#\partial A)}|X'_A|^{(-1)}$. Here $\#A$ is the number of the sites belonging to A, and $\#\partial A$ is the number of sites belonging to the boundary of subsystems A and B. One can verify that the coefficient C_P vanishes when we calculate the topological Rényi entropy Eq. (9). According to Eq. (A47), the last phase term $\sum_{\partial\bar{g}\in\partial G'_B}(-1)^{\partial\bar{g}\partial\bar{x}(\partial\bar{g})\cap\tilde{z}\tilde{h}}$ selects some particular $\tilde{z}\tilde{h}$ out. They satisfy the condition $[\partial\bar{g}\partial\bar{x}(\partial\bar{g}),\tilde{z}\tilde{h}] = 0$ for all the $\partial\bar{g} \in \partial G'_B$.

Exploiting the fact that in the τ picture, state $|\psi\rangle,|\phi\rangle$ and the operators occurred in Eq. (A54) have the tensor product form, we can decompose the purity as the product of each row and write Eq. (A54) in the form

$$P = C_P \prod_{k=1}^{R+2} \sum_{\partial\tilde{g}_{2k-1}\in\partial G'_{A_{2k-1}}} \sum_{\tilde{z}_{2k-1}\in Z'_{2k-1}} P_{2k-1}(\partial\tilde{g}_{2k-1},\tilde{z}_{2k-1}) \times \sum_{\tilde{h}_{2k}\in H'_{2k}} P_{2k}(\partial\tilde{x}_{2k}(\partial\tilde{g}_{2k-1},\partial\tilde{g}_{2k+1}),\tilde{h}_{2k}) \times \sum_{\partial\bar{g}_{2k-1}\in\partial G'_{B_{2k-1}}} (-1)^{\partial\bar{g}_{2k-1}\partial\bar{x}_{2k}(\partial\bar{g}_{2k-1},\partial\bar{g}_{2k+1})\cap\tilde{z}_{2k-1}\tilde{h}_{2k}}, \quad \text{(A55)}$$

where

$$P_{2k-1}(\partial\tilde{g}_{2k-1},\tilde{z}_{2k-1}) = \sum_{\tilde{g}_{2k-1}\in G'_{A_{2k-1}}} |\langle\psi_{2k-1}|\tilde{g}_{2k-1}\partial\tilde{g}_{2k-1}\tilde{z}_{2k-1}|\psi_{2k-1}\rangle|^2, \quad \text{(A56)}$$

$$P_{2k}(\partial\tilde{x}_{2k}(\partial\tilde{g}_{2k-1},\partial\tilde{g}_{2k+1}),\tilde{h}_{2k}) = \sum_{\tilde{x}_{2k}\in X'_{A_{2k}}} |\langle\phi_{2k}|\tilde{x}_{2k}\partial\tilde{x}_{2k}(\partial\tilde{g}_{2k-1},\partial\tilde{g}_{2k+1})\tilde{h}_{2k}|\phi_{2k}\rangle|^2. \quad \text{(A57)}$$

We illustrate how to proceed with the calculation by the case of subsystem type (1). We start from $k = 1$. The components of $\partial G'_A$ on the first row are $\mathbb{1}_1$, while $\partial G'_B$ is $\partial G'_{B_1}$. Omitting the constant coefficient, the $k = 1$ component of the purity is

$$P(k=1) = \sum_{\tilde{z}_1\in Z'_1} P_1(\tilde{z}_1) \sum_{\tilde{h}_2\in H'_{A_2}} P_2(\tilde{h}_2) \sum_{\partial\bar{g}_1\in\partial G'_{B_1}} (-1)^{\partial\bar{g}_1\partial\bar{x}_2(\partial\bar{g}_1)\cap\tilde{z}_1\tilde{h}_2}. \quad \text{(A58)}$$

The constraint of $[\partial\bar{g}_1\partial\bar{x}_2(\partial\bar{g}_1),\tilde{z}_1\tilde{h}_2] = 0$ directly gives that the summations of $\sum_{\tilde{z}_1\in Z'_1}$ and $\sum_{\tilde{h}_2\in H'_{A_2}}$ are not independent. Notice that $\partial\bar{g}_1\partial\bar{x}_2(\partial\bar{g}_1)$ constitutes a group and it is generated by $\tau^z_{s_j^1}\tau^x_{s_j^2}\tau^x_{s_{j+1}^2}$ in τ picture. The fact that $[\tau^z_{s_j^1}\tau^x_{s_j^2}\tau^x_{s_{j+1}^2},\tau^x_{s_j^1}\tau^x_{s_{j+1}^1}\tau^z_{s_j^2}] = 0$ tells us that $\tau^x_{s_j^1}\tau^x_{s_{j+1}^1}$ and $\tau^z_{s_j^2}$ always appear at the same time. Thus, $\tilde{h}_2$ is the function of $\tilde{z}_1$ and Eq. (A58) is

$$P(k=1) = \sum_{\tilde{z}_1\in Z'_1} P_1(\tilde{z}_1)P_2(\tilde{h}_2(\tilde{z}_1)). \quad \text{(A59)}$$

Next, we consider the $k = 2,\ldots,r+1$ case in which $\partial G'_{A_{2k-1}}$ and $\partial G'_{B_{2k-1}}$ contain only identity $\mathbb{1}_{2k-1}$ so the component of purity for this part is

$$P(k=2,\ldots,r+1) = \prod_{k=2}^{r}\left[\sum_{\tilde{z}_{2k-1}\in Z'_{2k-1}} P_{2k-1}(\tilde{z}_{2k-1})\right] \times \left[\sum_{\tilde{h}_{2k}\in H'_{A_{2k}}} P_{2k}(\tilde{h}_{2k})\right] P_{2r+1}(\tilde{z}_{2r+1}). \quad \text{(A60)}$$

It is clear that every row is independent with each other. Our aim is to get the topological Rényi entropy $S_2^T = \log_2(P^{(1)}P^{(4)}/P^{(2)}P^{(3)})$ and we can finally find that $P(k = 1,\ldots,r+1) = P(k=1)P(k=2,\ldots,r+1)$ for subsystem (1) is canceled during the calculation. The parts we are really concerned about are the rows which contain a "hole." We can write the purity of subsystem (1) as $P^{(1)} = P_{\text{top}}P^{(1)}_{\text{hole}}P_{\text{bottom}}$, where $P_{\text{top}} = P_{\text{bottom}} = P(k = 1,\ldots,r+1)$(caused by the symmetry of the subsystem and the fields). For subsystems (2) and (3) they are $P^{(2)} = P_{\text{top}}P^{(2)}_{\text{hole}}$ and $P^{(3)} = P^{(2)}_{\text{hole}}P_{\text{bottom}}$. For subsystem (4), every row contains a hole so $S_2^T = \log_2(P^{(1)}_{\text{hole}}P^{(4)}/P^{(2)}_{\text{hole}}P^{(3)}_{\text{hole}})$. We take subsystem (1), for

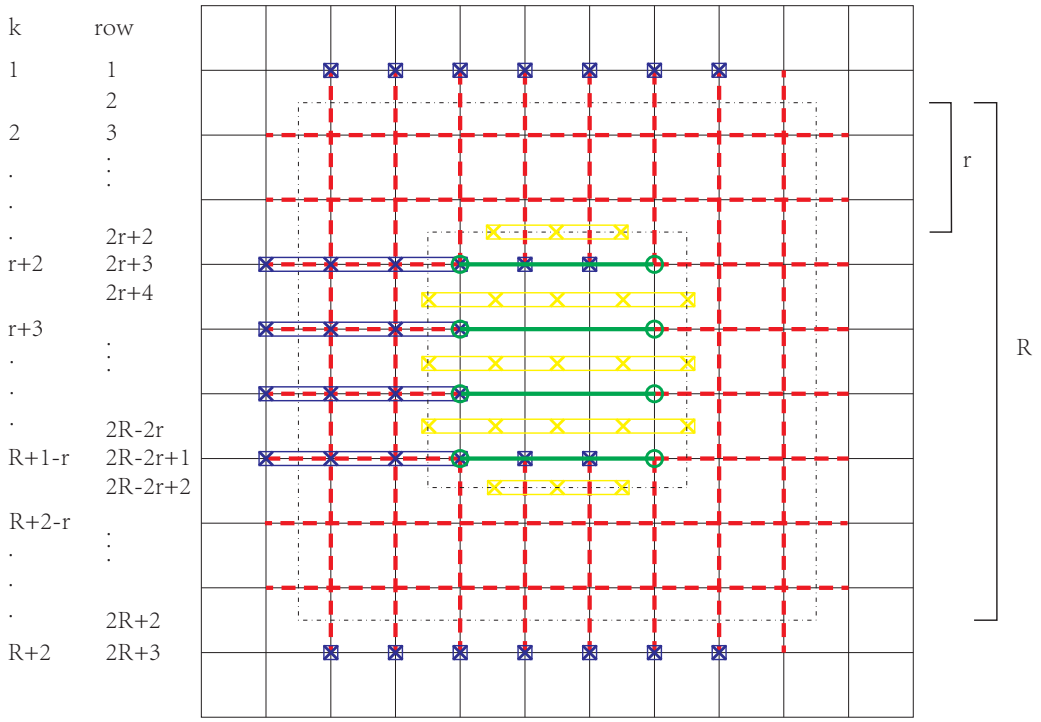

FIG. 8. Illustration of $\tilde{h}^c_{2k}$ (yellow rectangle blocks with crosses) and $\tilde{z}^c_{2k-1}$ (green solid lines with circular ends) in subsystem (1) with $R = 8, r = 2$.

example, to calculate $P^{(1)}_{\text{hole}}$:

$$P^{(1)}_{\text{hole}} = \prod_{k=r+2}^{R+1-r} \sum_{\partial\tilde{g}_{2k-1}} P_{2r+2}(\partial\tilde{x}_{2r+2}(\partial\tilde{g}_{2r+3}),\tilde{h}_{2r+2}) \times \sum_{\tilde{z}_{2k-1}} P_{2k-1}(\partial\tilde{g}_{2k-1},\tilde{z}_{2k-1}) \times \sum_{\tilde{h}_{2k}} P_{2k}(\partial\tilde{x}_{2k}(\partial\tilde{g}_{2k-1},\partial\tilde{g}_{2k+1}),\tilde{h}_{2k}) \times \sum_{\prod_{k=r+2}^{R+1-r}\partial\tilde{g}_{2k-1}} (-1)^{\partial\tilde{x}_{2r+2}\prod_{k=r+2}^{R+1-r}\partial\tilde{g}_{2k-1}\partial\tilde{x}_{2k}\cap\tilde{h}_{2r+2}\prod_{k=r+2}^{R+1-r}\tilde{z}_{2k-1}\tilde{h}_{2k}}. \tag{A61}$$

We use the the shorthand notation to denote the last phase term:

$$\sum_{\partial\tilde{g}_h}(-1)^{\partial\tilde{g}_h\partial\tilde{x}(\tilde{g}_m)\cap\tilde{z}_m\tilde{h}_m}. \tag{A62}$$

It gives a constraint in order to fulfill this term being nonzero. Showing as Figs. 7 and 8, the constraint is caused by $\partial\tilde{g}_h$ of types (ii) and (iii). We denote $\prod_{j=1}^{r+2}\tau^z_{s^{2k-1}_j}$ as $\partial\tilde{g}^c_{2k-1}$ (blue rectangle blocks), $\prod_{j=r+2}^{R-r}\tau^z_{s^{2k}_j}$ as $\tilde{h}^c_{2k}$ (yellow rectangle blocks) and $\tau^x_{s^{2k-1}_{r+2}}\tau^x_{s^{2k-1}_{R+1-r}}$ as $\tilde{z}^c_{2k-1}$ (green solid lines with cross ends). Notice the following relationship: $\{\partial\tilde{g}^c_{2k-1},\tilde{z}^c_{2k-1}\} = 0, \{\partial\tilde{x}(\partial\tilde{g}^c_{2k-1}),\tilde{h}^c_{2k-2}\} = 0$ and $\{\partial\tilde{x}(\partial\tilde{g}^c_{2k-1}),\tilde{h}^c_{2k}\} = 0$. We can get that for $k = (r+2),\ldots,(R+1-r)$, every $(\tilde{h}^c_{2k-2})^{m_{2k-2}}(\tilde{z}^c_{2k-1})^{m_{2k-1}}(\tilde{h}^c_{2k})^{m_{2k}}$ should obey $(m_{2k-2}+m_{2k-1}+m_{2k})\text{mod}2 = 0$ ($\{m\} = 0,1$). The number of possible configuration is $2^{(R-2r+1)}$. We choose $R = 5, r = 1$, for example, then the number is 16. Every Column in the Table II represents one possible configuration $\{m\}$.

We denote $\sum_{\{\tilde{z},\tilde{h}\}_{\text{constr.}}}$ as the summation of $\tilde{z},\tilde{h}$ in all the possible configurations, which satisfy the constraint. Finally, we get

$$P^{(1)}_{\text{hole}} = C^{(1)}_{\text{hole}} \prod_{k=r+2}^{R+1-r} \sum_{\partial\tilde{g}_{2k-1}} \sum_{\{\tilde{z},\tilde{h}\}_{\text{constr.}}} P_{2r+2}(\partial\tilde{x}_{2r+2}(\partial\tilde{g}_{2r+3}),\tilde{h}_{2r+2}) \times P_{2k-1}(\partial\tilde{g}_{2k-1},\tilde{z}_{2k-1})P_{2k}(\partial\tilde{x}_{2k}(\partial\tilde{g}_{2k-1},\partial\tilde{g}_{2k+1}),\tilde{h}_{2k}). \tag{A63}$$

The coefficient comes from Eq. (A47) and it is vanished when we calculate the topological Rényi entropy. Together with Eq. (A56) and (A57), the final task is to calculate the modulus square expectation values in form of $|\langle\psi|\tau^z_{m_1}\cdots\tau^z_{m_s}\cdots\tau^x_{n_1}\cdots\tau^x_{n_{2t}}|\psi\rangle|^2$ for each row. We are concerned with the state $|\psi\rangle$ in two conditions: (i) the static one, which is the ground state of the Ising Hamiltonian shown

TABLE II. All possible configurations of $\{m\}$ obeying $(m_{2k-2}+m_{2k-1}+m_{2k})\text{mod}2 = 0$ for $k = (r+2),\ldots,(R+1-r)$, with subsystem size $R = 5, r = 1$.

m_4	0	0	0	0	0	0	0	0	1	1	1	1	1	1	1	1
m_5	0	0	0	0	1	1	1	1	0	0	0	0	1	1	1	1
m_6	0	0	0	0	1	1	1	1	1	1	1	1	0	0	0	0
m_7	0	0	1	1	0	0	1	1	0	0	1	1	0	0	1	1
m_8	0	0	1	1	1	1	0	0	1	1	0	0	0	0	1	1
m_9	0	1	0	1	0	1	0	1	0	1	0	1	0	1	0	1
m_{10}	0	1	1	0	1	0	0	1	1	0	0	1	0	1	1	0

in Eq. (A5) for each row; (ii) time evolution state after a quantum quench. Both of them can be treated analytically in free fermion representation.

3. Calculation of purity: Mapping to free fermions

As we saw in the previous section, the purity P can then be directly calculated in terms of expectation values of strings of τ operators. These expectation values can be computed exactly in the case of the integrable chain [83,103]. We are concerned with one-dimensional Ising model in the transverse field:

$$H_{\text{Ising}} = -\sum_{l=1}^{N}\left(\tau_l^z + \lambda\tau_l^x\tau_{l+1}^x\right). \tag{A64}$$

We take the standard procedure of Jordan-Wigner transformation to map the Hamiltonian to the free fermion representation:

$$\tau_l^z = 1 - 2c_l^\dagger c_l, \quad \tau_l^+ = (\tau_l^-)^\dagger = \prod_{j=1}^{l-1}(1-2c_j^\dagger c_j)c_l. \tag{A65}$$

Note that we map the spin-up state $|\uparrow\rangle$ to the vacuum $|0\rangle$. So the spin Hamiltonian transforms to the fermion Hamiltonian

$$\begin{aligned} H_{Ising} = &-\sum_{l=1}^{N}(c_l^\dagger + c_l)(c_l^\dagger - c_l) - \lambda\sum_{l=1}^{N}(c_l^\dagger - c_l)(c_{l+1}^\dagger + c_{l+1}) \\ &+\lambda\left[\exp\left(i\pi\sum_{j=1}^{n}c_j^\dagger c_j\right)+1\right](c_N^\dagger - c_N)(c_1^\dagger + c_1). \end{aligned} \tag{A66}$$

Notice that the operator identity $1-2c_j^\dagger c_j = (c_j^\dagger + c_j)(c_j^\dagger - c_j) = \exp(i\pi c_j^\dagger c_j)$ and the term $\exp(i\pi\sum_{j=1}^{n}c_j^\dagger c_j)$ is actually the parity operator of the system, which is 1 in the subspace we choose. Nevertheless, the last term is the correction term, which we neglect in the large N limit. As the former formula showed, what we are interested in are modulus square expectation values, written as $|\langle\psi|\tau_{m_1}^z\cdots\tau_{m_s}^z\cdots\tau_{n_1}^x\cdots\tau_{n_{2t}}^x|\psi\rangle|^2$. Defining $A_j = c_j^\dagger + c_j$, $B_j = c_j^\dagger - c_j$, it is easy to check that $\tau_j^z = A_jB_j$ and $\tau_j^x\tau_{j+1}^x = B_jA_{j+1}$. Noting that $A_j^2 = 1$ and $B_j^2 = -1$, the former equation can be written in the form of $|\langle\psi|\cdots A_s\cdots B_t\cdots|\psi\rangle|^2$. Wick's theorem tells us this expression can be reduced to the product of two-operator expectation values.

Applying Fourier transformation

$$c_l = \frac{1}{\sqrt{N}}\sum_q e^{iql}c_q, \tag{A67}$$

the Hamiltonian is rewritten in momentum space as

$$\begin{aligned} H &= \sum_q(1-\lambda\cos q)(c_q^\dagger c_q - c_{-q}c_{-q}^\dagger) \\ &\quad -\lambda i\sum_q \sin q(c_q^\dagger c_{-q}^\dagger - c_{-q}c_q) \\ &= \sum_q C_q^\dagger M_q(\lambda)C_q, \end{aligned} \tag{A68}$$

where

$$\begin{aligned} M_q(\lambda) &= \begin{pmatrix} a_q(\lambda) & -ib_q(\lambda) \\ ib_q(\lambda) & -a_q(\lambda)\end{pmatrix}, \\ a_q(\lambda) &= 1-\lambda\cos q, \quad b_q(\lambda) = \lambda\sin q, \end{aligned} \tag{A69}$$

and

$$C_q = \begin{pmatrix} c_q \\ c_{-q}^\dagger\end{pmatrix}. \tag{A70}$$

The Hamiltonian is diagonalized by the Bogoliubov transformation,

$$H = \sum_q h_q(\lambda)^\dagger\begin{pmatrix}\omega_q(\lambda) & 0 \\ 0 & -\omega_q(\lambda)\end{pmatrix}h_q(\lambda), \tag{A71}$$

where

$$\begin{aligned} h_q(\lambda) &= \begin{pmatrix}\eta_q(\lambda) \\ \eta_{-q}^\dagger(\lambda)\end{pmatrix} = R_q^\dagger(\lambda)C_q, \\ R_q(\lambda) &= \begin{pmatrix} u_q(\lambda) & -iv_q(\lambda) \\ -iv_q(\lambda) & u_q(\lambda)\end{pmatrix}, \end{aligned} \tag{A72}$$

with

$$\begin{aligned} u_q(\lambda) &= \frac{a_q(\lambda)+\omega_q(\lambda)}{\sqrt{2\omega_q(\lambda)[\omega_q(\lambda)+a_q(\lambda)]}}, \\ v_q(\lambda) &= \frac{-b_q(\lambda)}{\sqrt{2\omega_q(\lambda)[\omega_q(\lambda)+a_q(\lambda)]}}, \end{aligned} \tag{A73}$$

and

$$\omega_q(\lambda) = \sqrt{a_q(\lambda)^2 + b_q(\lambda)^2} = \sqrt{1-2\lambda\text{cosq}+\lambda^2}. \tag{A74}$$

After diagonalizing the Hamiltonian, we can obtain the exact eigenstates. Moreover, we can obtain an exact expression for the time evolution. In the quantum quench scenario, the state evolves as

$$|\Psi(t)\rangle = U(t)|\Psi(0)\rangle = e^{-itH(\lambda(t))}|\Psi(0)\rangle, \tag{A75}$$

in which

$$\lambda(t) = \begin{cases}\lambda_0 & (t\leqslant 0), \\ \lambda & (t>0),\end{cases} \tag{A76}$$

and the initial state $|\Psi(0)\rangle$ is the ground state of $H(\lambda_0)$, namely, $\eta_q(\lambda_0)|\Psi(0)\rangle = 0, \forall\, q$. (Basically what we are interested in is the condition of $\lambda_0 = 0$ in which the following derivation would be simplified, but we do the derivation in general condition.) We need to calculate the expectation value of $\langle\Psi(t)|O|\Psi(t)\rangle = \langle\Psi(0)|e^{itH(\lambda(t))}Oe^{-itH(\lambda(t))}|\Psi(0)\rangle = \langle\Psi(0)|O^H(t)|\Psi(0)\rangle$, and operator O we are concerned with is the product of some A_j and B_k operators. So we need to apply the Wick's theorem in Heisenberg picture. First we focus on $c_q^H(t)$ whose Heisenberg equation is

$$\begin{aligned} i\frac{d}{dt}c_q^H(t) &= U^\dagger(t)[c_q, H(\lambda(t))]U(t) \\ &= 2a_q(\lambda(t))c_q^H(t) - 2ib_q(\lambda(t))c_{-q}^H(t)^\dagger, \end{aligned} \tag{A77}$$

or more compactly,

$$i\frac{d}{dt}C_q^H(t) = 2M_q(\lambda(t))C_q^H(t), \tag{A78}$$

where $M_q(\lambda(t))$ has the same form of Eq. (A69). Expand $C_q^H(t)$ by $\eta_q(\lambda_0)$ and $\eta_{-q}^\dagger(\lambda_0)$ as $C_q^H(t) = S_q(t)h_q(\lambda_0)$;

thus,

$$S_q(t)=\begin{pmatrix}\tilde{u}_q(t) & -\tilde{v}_q^*(t)\\ \tilde{v}_q(t) & \tilde{u}_q^*(t)\end{pmatrix}, \tag{A79}$$

which is unitary and obeys the constraints

$$\tilde{u}_q(t)=\tilde{u}_{-q}(t),\quad \tilde{v}_q(t)=-\tilde{v}_{-q}(t). \tag{A80}$$

Then we obtain equations of motion for $S_q(t)$:

$$i\frac{d}{dt}\begin{pmatrix}\tilde{u}_q(t)\\ \tilde{v}_q(t)\end{pmatrix}=2\begin{pmatrix}a_q(\lambda(t)) & -ib_q(\lambda(t))\\ ib_q(\lambda(t)) & -a_q(\lambda(t))\end{pmatrix}\begin{pmatrix}\tilde{u}_q(t)\\ \tilde{v}_q(t)\end{pmatrix}. \tag{A81}$$

The solution is given by

$$\begin{pmatrix}\tilde{u}_q(t)\\ \tilde{v}_q(t)\end{pmatrix}=R_q(\lambda)\begin{pmatrix}e^{-i2\omega_q(\lambda)t} & 0\\ 0 & e^{i2\omega_q(\lambda)t}\end{pmatrix}R_q^\dagger(\lambda)\begin{pmatrix}\tilde{u}_q(0)\\ \tilde{v}_q(0)\end{pmatrix}, \tag{A82}$$

and the initial condition is given by

$$\begin{pmatrix}\tilde{u}_q(0)\\ \tilde{v}_q(0)\end{pmatrix}=\begin{pmatrix}u_q(\lambda_0)\\ -iv_q(\lambda_0)\end{pmatrix}, \tag{A83}$$

which comes from the identity of $S_q(t=0)=R_q(\lambda_0)$, seeing Eqs. (A72) and (A79). Substituting Eq. (A73) into (A82), the solution can be written explicitly as

$$\begin{pmatrix}\tilde{u}_q(t)\\ \tilde{v}_q(t)\end{pmatrix}=\begin{pmatrix}u_0\cos 2\omega t+i\left(\frac{-au_0+bv_0}{\omega}\right)\sin 2\omega t\\ -iv_0\cos 2\omega t+\left(\frac{bu_0+av_0}{\omega}\right)\sin 2\omega t\end{pmatrix}, \tag{A84}$$

where we have applied the shorthand notations $a=a_q(\lambda)$, $b=b_q(\lambda)$, $\omega=\omega_q(\lambda)$, $u_0=u_q(\lambda_0)$, and $v_0=v_q(\lambda_0)$.

It is the time to work on the operators $A_j^H(t)$ and $B_j^H(t)$. As the standard procedure of applying Wick's theorem, we need to decompose the operators in two parts: $A_j^H(t)=a_j^\dagger(t)+a_j(t)$ and $B_j^H(t)=b_j^\dagger(t)-b_j(t)$, where

$$a_j(t)=\frac{1}{\sqrt{N}}\sum_q e^{iqj}[\tilde{u}_q(t)+\tilde{v}_q(t)]\eta_q(\lambda_0),$$

$$b_j(t)=\frac{1}{\sqrt{N}}\sum_q e^{iqj}[\tilde{u}_q(t)-\tilde{v}_q(t)]\eta_q(\lambda_0). \tag{A85}$$

Notice that $a_j(t)$ [also $b_j(t)$] is a combination of $\eta_q(\lambda_0)$, which are the destruction operators acting on the initial state $|\Psi(0)\rangle$, while $a_j^\dagger(t)$ [also $b_j^\dagger(t)$] is a combination of $\eta_q^\dagger(\lambda_0)$.

Actually, $\{\eta_q(\lambda_0)\}$ and $\{\eta_q^\dagger(\lambda_0)\}$ form a set of bases of the operators in the Hilbert space, so any operator O has a decomposition $O=O^-+O^+$, where $O^-|\Psi(0)\rangle=0$ and $\langle\Psi(0)|O^+=0$. A two-operator product can be written as $O_1O_2=N[O_1O_2]+\{O_1^-,O_2^+\}$, where N is the normal ordering operator and the anticommutator comes from the Fermi statistics. So the expectation value satisfies $\langle\Psi(0)|O_1O_2|\Psi(0)\rangle=\{O_1^-,O_2^+\}$, which is known as contraction of two operators.

The following three types of contraction are concerned:

$$G_{j-k}(t)=\langle\Psi(0)|A_j^H(t)B_k^H(t)|\Psi(0)\rangle=\{a_j(t),b_k^\dagger(t)\},$$

$$G_{j-k}^A(t)=\langle\Psi(0)|A_j^H(t)A_k^H(t)|\Psi(0)\rangle=\{a_j(t),a_k^\dagger(t)\},$$

$$G_{j-k}^B(t)=\langle\Psi(0)|B_j^H(t)B_k^H(t)|\Psi(0)\rangle=-\{b_j(t),b_k^\dagger(t)\}. \tag{A86}$$

Substituting (A85), they can be written explicitly as

$$\begin{aligned}G_{j-k}(t)&=\frac{1}{N}\sum_q e^{iq(j-k)}[|\tilde{u}_q(t)|^2-|\tilde{v}_q(t)|^2\\&\quad+\tilde{v}_q(t)\tilde{u}_q^*(t)-\tilde{u}_q(t)\tilde{v}_q^*(t)],\\ G_{j-k}^A(t)&=\delta_{j,k}+\frac{1}{N}\sum_q e^{iq(j-k)}[\tilde{v}_q(t)\tilde{u}_q^*(t)+\tilde{u}_q(t)\tilde{v}_q^*(t)],\\ G_{j-k}^B(t)&=-\delta_{j,k}+\frac{1}{N}\sum_q e^{iq(j-k)}[\tilde{v}_q(t)\tilde{u}_q^*(t)+\tilde{u}_q(t)\tilde{v}_q^*(t)].\end{aligned} \tag{A87}$$

Noticing that $G_{j-k}^*(t)=G_{j-k}(t)$, so the contraction $\langle B_j^H(t)A_k^H(t)\rangle=-\langle A_k^H(t)B_j^H(t)\rangle^*=-G_{-(j-k)}$.

Substituting Eq. (A84) into Eqs. (A87) and replacing $j-k$ with r, we can get the final contraction formulas:

$$\begin{aligned}G_r(t)&=\frac{1}{N}\sum_q e^{iqr}\left[\frac{a_0a+b_0b}{(a-ib)\omega_0}+i\cos 4\omega t\frac{ab_0-a_0b}{(a-ib)\omega_0}\right],\\ G_r^A(t)&=\delta_{r,0}+\frac{1}{N}\sum_q e^{iqr}\left(\frac{-ab_0+a_0b}{\omega\omega_0}\right)\sin 4\omega t,\\ G_r^B(t)&=-\delta_{r,0}+\frac{1}{N}\sum_q e^{iqr}\left(\frac{-ab_0+a_0b}{\omega\omega_0}\right)\sin 4\omega t.\end{aligned} \tag{A88}$$

In the end, we discuss the formulas in two special cases.

(1) Static case. In this case $\lambda_0=\lambda$ and the initial state (eigenstate of the quench Hamiltonian) will stay unchanged. So we have $a_0=a=a_q(\lambda)=1-\lambda\cos q$, $b_0=b=b_q(\lambda)=\lambda\sin q$, and $\omega_0=\omega=\omega_q(\lambda)=\sqrt{1-2\lambda\cos q+\lambda^2}$. It gives the contraction formulas in static case directly:

$$\begin{aligned}G_r&=\frac{1}{N}\sum_q e^{iqr}\left(\frac{a-ib}{\omega}\right)\\&=\frac{1}{N}\sum_q e^{iqr}\left(\frac{1-\lambda e^{iq}}{\sqrt{1-2\lambda\cos q+\lambda^2}}\right),\\ G_r^A&=\delta_{r,0},\quad G_r^B=-\delta_{r,0}.\end{aligned} \tag{A89}$$

The time-dependent terms vanish automatically during the derivation in this condition.

(2) Quantum quench ($N\to\infty$,$t\to\infty$) case. Basically, we consider that the initial state is the ground state of the toric code model, which corresponds to $\lambda_0=0$. In this case we have $a_0=1$, $b_0=0$, and $\omega_0=1$. We are concerned with long-time evolution in this paper, so the limit $t\to\infty$ is reasonable. Taking the thermodynamic limit $\frac{1}{N}\sum_q\to\int dq/2\pi$, the time-dependent term vanishes caused by the fast oscillation of the integrand. Thus, we can get

$$G_r(\infty)=\frac{1}{2\pi}\int_{-\pi}^{\pi}dqe^{iqr}\frac{a}{(a-ib)}. \tag{A90}$$

Remembering that $a=a_q(\lambda)=1-\lambda\cos q$ and $b=b_q(\lambda)=\lambda\sin q$, so

$$G_r(\infty)=\frac{1}{2\pi}\int_{-\pi}^{\pi}dqe^{-iqr}\frac{2-\lambda(e^{iq}+e^{-iq})}{2(1-\lambda e^{-iq})}. \tag{A91}$$

Changing the integral to a contour integral on the complex plane of $z = e^{iq}$,

$$G_r(\infty) = \frac{1}{2\pi i}\oint dz z^{-r-1}\frac{-\lambda z^2 + 2z - \lambda}{2(z-\lambda)}, \tag{A92}$$

where the integral path is along the unit circle. Applying the residue theorem we can finally obtain the exact value of $G_r(\infty)$. For $\lambda < 1$,

$$G_r(\infty) = \begin{cases} 0 & (r \geqslant 2), \\ -\lambda/2 & (r = 1), \\ -\frac{1}{2}\lambda^2 + 1 & (r = 0), \\ \frac{1}{2}\lambda^{-r}(1-\lambda^2) & (r \leqslant -1), \end{cases} \tag{A93}$$

and for $\lambda > 1$,

$$G_r(\infty) = \begin{cases} \frac{1}{2}\lambda^{-r}(\lambda^2 - 1) & (r \geqslant 2), \\ -\frac{1}{2\lambda} & (r = 1), \\ \frac{1}{2} & (r = 0), \\ 0 & (r \leqslant -1). \end{cases} \tag{A94}$$

We can also get $G_r^A(\infty) = \delta_{r,0}$ and $G_r^B(\infty) = -\delta_{r,0}$; thus, all types of contraction are known. The modulus square of the expectation value $|\langle\Psi(t)|\cdots A_s \cdots B_t \cdots |\Psi(t)\rangle|^2$ can be directly calculated.

[1] S. Sachdev, *Quantum Phase Transitions* (Cambridge University Press, Cambridge, UK, 1999).

[2] X. G. Wen, *Quantum Field Theory of Many Body Systems* (Oxford University Press, Oxford, UK, 2004).

[3] M. Greiner, O. Mandel, T. Esslinger, T. W. Hänsch, and I. Bloch, Quantum phase transition from a superfluid to a Mott insulator in a gas of ultracold atoms, Nature (London) **415**, 39 (2002).

[4] M. Greiner, O. Mandel, T. W. Hänsch, and I. Bloch, Collapse and revival of the matter wave field of a Bose-Einstein condensate, Nature (London) **419**, 51 (2002).

[5] I. Bloch, J. Dalibard, and W. Zwerger, Many-body physics with ultracold gases, Rev. Mod. Phys. **80**, 885 (2008).

[6] A. Polkovnikov, K. Sengupta, A. Silva, and M. Vengalattore, Colloquium: Nonequilibrium dynamics of closed interacting quantum systems, Rev. Mod. Phys. **83**, 863 (2011).

[7] N. Goldenfeld, *Lectures on Phase Transitions and the Renormalization Group* (Addison Wesley, New York, 1992).

[8] X. G. Wen and Q. Niu, Ground-state degeneracy of the fractional quantum Hall states in the presence of a random potential and on high-genus Riemann surfaces, Phys. Rev. B **41**, 9377 (1990).

[9] Z. Nussinov and G. Ortiz, A symmetry principle for topological quantum order, Ann. Phys. (NY) **324**, 977 (2009).

[10] Z. Nussinov and G. Ortiz, Autocorrelations and thermal fragility of anyonic loops in topologically quantum ordered systems, Phys. Rev. B **77**, 064302 (2008).

[11] M. H. Freedman, A. Kitaev, and Z. Wang, Simulation of topological field theories by quantum computers, Commun. Math. Phys. **227**, 587 (2002).

[12] A. Hamma, R. Ionicioiu, and P. Zanardi, Ground state entanglement and geometric entropy in the Kitaev model, Phys. Lett. A **337**, 22 (2005).

[13] A. Hamma, R. Ionicioiu, and P. Zanardi, Bipartite entanglement and entropic boundary law in lattice spin systems, Phys. Rev. A **71**, 022315 (2005).

[14] A. Kitaev and J. Preskill, Topological Entanglement Entropy, Phys. Rev. Lett. **96**, 110404 (2006).

[15] M. Levin and X.-G. Wen, Detecting Topological Order in a Ground State Wave Function, Phys. Rev. Lett. **96**, 110405 (2006).

[16] I. H. Kim, Long-Range Entanglement Is Necessary for a Topological Storage of Quantum Information, Phys. Rev. Lett. **111**, 080503 (2013).

[17] S. Trebst, P. Werner, M. Troyer, K. Shtengel, and C. Nayak, Breakdown of a Topological Phase: Quantum Phase Transition in a Loop Gas Model with Tension, Phys. Rev. Lett. **98**, 070602 (2007).

[18] S. Isakov, M. Hastings, and R. Melko, Topological entanglement entropy of a Bose-Hubbard spin liquid, Nat. Phys. **7**, 772 (2011).

[19] S. Papanikolaou, K. S. Raman, and E. Fradkin, Topological phases and topological entropy of two-dimensional systems with finite correlation length, Phys. Rev. B **76**, 224421 (2007).

[20] A. Hamma, R. Ionicioiu, and P. Zanardi, Quantum entanglement in states generated by bilocal group algebras, Phys. Rev. A **72**, 012324 (2005).

[21] Y. A. Lee and G. Vidal, Entanglement negativity and topological order, Phys. Rev. A **88**, 042318 (2013).

[22] C. Castelnovo, Negativity and topological order in the toric code, Phys. Rev. A **88**, 042319 (2013).

[23] T. Grover, A. M. Turner, and A. Vishwanath, Entanglement entropy of gapped phases and topological order in three dimensions, Phys. Rev. B **84**, 195120 (2011).

[24] A. Hamma, W. Zhang, S. Haas, and D. A. Lidar, Entanglement, fidelity, and topological entropy in a quantum phase transition to topological order, Phys. Rev. B **77**, 155111 (2008).

[25] E. Dennis, A. Kitaev, A. Landahl, and J. Preskill, Topological quantum memory, J. Math. Phys. **43**, 4452 (2002).

[26] D. Mazáč and A. Hamma, Topological order, entanglement, and quantum memory at finite temperature, Ann. Phys. (NY) **327**, 2096 (2012).

[27] S. Bravyi and B. Terhal, A no-go theorem for a two-dimensional self-correcting quantum memory based on stabilizer codes, New J. Phys. **11**, 043029 (2009).

[28] J. K. Pachos and S. H. Simon, Focus on topological quantum computation, New J. Phys. **16**, 065003 (2014).

[29] C. Nayak, S. H. Simon, A. Stern, M. Freedman, and S. Das Sarma, Non-Abelian anyons and topological quantum computation, Rev. Mod. Phys. **80**, 1083 (2008).

[30] S. Das Sarma, M. Freedman, and C. Nayak, Topologically Protected Qubits from a Possible Non-Abelian Fractional Quantum Hall State, Phys. Rev. Lett. **94**, 166802 (2005).

[31] A. Y. Kitaev, Fault-tolerant quantum computation by anyons, Ann. Phys. (NY) **303**, 2 (2003).

[32] A. K. Chandra, A. Das, and B. K. Chakrabarti (eds.), *Quantum Quenching, Annealing and Computation* (Springer, Heidelberg, 2010).

[33] S. V. Isakov, P. Fendley, A. W. W. Ludwig, S. Trebst, and M. Troyer, Dynamics at and near conformal quantum critical points, Phys. Rev. B **83**, 125114 (2011).

[34] A. Rahmani and C. Chamon, Exact results on the quench dynamics of the entanglement entropy in the toric code, Phys. Rev. B **82**, 134303 (2010).

[35] P. Calabrese and J. Cardy, Time Dependence of Correlation Functions Following a Quantum Quench, Phys. Rev. Lett. **96**, 136801 (2006).

[36] M. A. Cazalilla, Effect of Suddenly Turning on Interactions in the Luttinger Model, Phys. Rev. Lett. **97**, 156403 (2006).

[37] M. Rigol, V. Dunjko, V. Yurovsky, and M. Olshanii, Relaxation in a Completely Integrable Many-Body Quantum System: An Ab Initio Study of the Dynamics of the Highly Excited States of 1D Lattice Hard-Core Bosons, Phys. Rev. Lett. **98**, 050405 (2007).

[38] S. S. Jahromi, M. Kargarian, S. F. Masoudi, and K. P. Schmidt, Robustness of a topological phase: Topological color code in a parallel magnetic field, Phys. Rev. B **87**, 094413 (2013).

[39] C. Castelnovo and C. Chamon, Quantum topological phase transition at the microscopic level, Phys. Rev. B **77**, 054433 (2008).

[40] G. B. Halász and A. Hamma, Probing topological order with Rényi entropy, Phys. Rev. A **86**, 062330 (2012).

[41] M. D. Schulz, S. Dusuel, R. Orus, J. Vidal, and K. P. Schmidt, Breakdown of a perturbed $\mathbb{Z}_N$ topological phase, New J. Phys. **14**, 025005 (2012).

[42] A. Hamma and D. A. Lidar, Adiabatic Preparation of Topological Order, Phys. Rev. Lett. **100**, 030502 (2008).

[43] J. Vidal, S. Dusuel, and K. P. Schmidt, Low-energy effective theory of the toric code model in a parallel magnetic field, Phys. Rev. B **79**, 033109 (2009).

[44] J. Vidal, R. Thomale, K. P. Schmidt, and S. Dusuel, Self-duality and bound states of the toric code model in a transverse field, Phys. Rev. B **80**, 081104(R) (2009).

[45] F. Wu, Y. Deng, and N. Prokof'ev, Phase diagram of the toric code model in a parallel magnetic field, Phys. Rev. B **85**, 195104 (2012).

[46] V. Karimipour, L. Memarzadeh, and P. Zarkeshian, Kitaev-Ising model and the transition between topological and ferromagnetic order, Phys. Rev. A **87**, 032322 (2013).

[47] A. Hamma, L. Cincio, S. Santra, P. Zanardi and, L. Amico, Local Response of Topological Order to an External Perturbation, Phys. Rev. Lett. **110**, 210602 (2013).

[48] L. Cincio and G. Vidal, Characterizing Topological Order by Studying the Ground States on an Infinite Cylinder, Phys. Rev. Lett. **110**, 067208 (2013).

[49] S. Bravyi, M. Hastings, and S. Michalakis, Topological quantum order: Stability under local perturbations, J. Math. Phys. **51**, 093512 (2010).

[50] S. Bravyi and M. Hastings, A short proof of stability of topological order under local perturbations, Commun. Math. Phys. **307**, 609 (2011).

[51] I. Klich, On the stability of topological phases on a lattice, Ann. Phys. (NY) **325**, 2120 (2010).

[52] M. Rigol, V. Dunjko, and M. Olshanii, Thermalization and its mechanism for generic isolated quantum systems, Nature (London) **452**, 854 (2008).

[53] J. M. Deutsch, Quantum statistical mechanics in a closed system, Phys. Rev. A **43**, 2046 (1991).

[54] M. Srednicki, Chaos and quantum thermalization, Phys. Rev. E **50**, 888 (1994).

[55] S. Popescu, A. J. Short, and A. Winter, Entanglement and the foundations of statistical mechanics, Nat. Phys. **2**, 754 (2006).

[56] N. Linden, S. Popescu, A. J. Short, and A. Winter, Quantum mechanical evolution towards thermal equilibrium, Phys. Rev. E **79**, 061103 (2009).

[57] C. Gogolin and J. Eisert, Equilibration, thermalisation, and the emergence of statistical mechanics in closed quantum systems, Rep. Prog. Phys. **79**, 056001 (2016).

[58] C. Castelnovo and C. Chamon, Topological order and topological entropy in classical systems, Phys. Rev. B **76**, 174416 (2007).

[59] C. Castelnovo and C. Chamon, Entanglement and topological entropy of the toric code at finite temperature, Phys. Rev. B **76**, 184442 (2007).

[60] C. Castelnovo and C. Chamon, Topological order in a three-dimensional toric code at finite temperature, Phys. Rev. B **78**, 155120 (2008).

[61] M. B. Hastings, Topological Order at Nonzero Temperature, Phys. Rev. Lett. **107**, 210501 (2011).

[62] G. B. Halász and A. Hamma, Topological Rényi Entropy after a Quantum Quench, Phys. Rev. Lett. **110**, 170605 (2013).

[63] A. Kay, Nonequilibrium Reliability of Quantum Memories, Phys. Rev. Lett **102**, 070503 (2009).

[64] G. Kells, D. Sen, J. K. Slingerland, and S. Vishveshwara, Topological blocking in quantum quench dynamics, Phys. Rev. B **89**, 235130 (2014).

[65] D. I. Tsomokos, A. Hamma, W. Zhang, S. Haas, and R. Fazio, Topological order following a quantum quench, Phys. Rev. A **80**, 060302(R) (2009).

[66] S. Santra, A. Hamma, L. Cincio, Y. Subasi, P. Zanardi, and L. Amico, Local convertibility of the ground state of the perturbed toric code, Phys. Rev. B **90**, 245128 (2014).

[67] H. D. Chen, and J. P. Hu, Exact mapping between classical and topological orders in two-dimensional spin systems, Phys. Rev. B **76**, 193101 (2007).

[68] X. Y. Feng, G. M. Zhang, and T. Xiang, Topological Characterization of Quantum Phase Transitions in a Spin-1/2 Model, Phys. Rev. Lett. **98**, 087204 (2007).
[69] J. Yu, S.-P. Kou, and X.-G. Wen, Topological quantum phase transition in the transverse Wen-plaquette model, Europhys. Lett. **84**, 17004 (2008).
[70] S. Dusuel, M. Kamfor, R. Orús, K. P. Schmidt, and J. Vidal, Robustness of a Perturbed Topological Phase, Phys. Rev. Lett. **106**, 107203 (2011).
[71] L. Amico, R. Fazio, A. Osterloh, and V. Vedral, Entanglement in many-body systems, Rev. Mod. Phys. **80**, 517 (2008).
[72] M. Nielsen and I. Chuang, *Quantum Computation and Quantum Information* (Cambridge University Press, Cambridge, UK, 2010).
[73] A. Hamma, S. Santra, and P. Zanardi, Quantum Entanglement in Random Physical States, Phys. Rev. Lett. **109**, 040502 (2012).
[74] V. Vedral, Quantifying entanglement in macroscopic systems, Nature (London) **453**, 1004 (2008).
[75] S. T. Flammia, A. Hamma, T. L. Hughes, and X.-G. Wen, Topological Entanglement Rényi Entropy and Reduced Density Matrix Structure, Phys. Rev. Lett. **103**, 261601 (2009).
[76] A. K. Ekert, C. M. Alves, D. K. L. Oi, M. Horodecki, P. Horodecki, and L. C. Kwek, Direct Estimations of Linear and Nonlinear Functionals of a Quantum State, Phys. Rev. Lett. **88**, 217901 (2002).
[77] D. A. Abanin and E. Demler, Measuring Entanglement Entropy of a Generic Many-Body System with a Quantum Switch, Phys. Rev. Lett. **109**, 020504 (2012).
[78] A. J. Daley, H. Pichler, J. Schachenmayer, and P. Zoller, Measuring Entanglement Growth in Quench Dynamics of Bosons in an Optical Lattice, Phys. Rev. Lett. **109**, 020505 (2012).
[79] R. Islam, R. Ma, P. M. Preiss, M. E. Tai, A. Lukin, M. Rispoli, and M. Greiner, Measuring entanglement entropy in a quantum many-body system, Nature (London) **528**, 77 (2015).
[80] M. Kamfor, S. Dusuel, J. Vidal, and K. P. Schmidt, Spectroscopy of a topological phase, Phys. Rev. B **89**, 045411 (2014).
[81] H. Wang, B. Bauer, M. Troyer, and V. W. Scarola, Identifying quantum topological phases through statistical correlation, Phys. Rev. B **83**, 115119 (2011).
[82] P. Pfeuty, The one-dimensional Ising model with a transverse field, Ann. Phys. (NY) **57**, 79 (1970).
[83] E. Barouch and B. M. McCoy, Statistical mechanics of the XY model. II. Spin-correlation functions, Phys. Rev. A **3**, 786 (1971).
[84] E. Lieb, T. Schultz, and D. Mattis, Two soluble models of an antiferromagnetic chain, Ann. Phys. (NY) **16**, 407 (1961).
[85] L. C. Venuti, The recurrence time in quantum mechanics, arXiv:1509.04352.
[86] J. Häppölä, G. B. Halász, and A. Hamma, Universality and robustness of revivals in the transverse field XY model, Phys. Rev. A **85**, 032114 (2012).
[87] S. Montes and A. Hamma, Phase diagram and quench dynamics of the cluster-XY spin chain, Phys. Rev. E **86**, 021101 (2012).
[88] E. H. Lieb and D. W. Robinson, The finite group velocity of quantum spin systems, Commun. Math. Phys. **28**, 251 (1972).
[89] B. Nachtergaele, Y. Ogata, and R. Sims, Propagation of correlations in quantum lattice systems, J. Stat. Phys. **124**, 1 (2006).
[90] S. Bravyi, M. B. Hastings, and F. Verstraete, Lieb-Robinson Bounds and the Generation of Correlations and Topological Quantum Order, Phys. Rev. Lett. **97**, 050401 (2006).
[91] J. Eisert and T. J. Osborne, General Entanglement Scaling Laws from Time Evolution, Phys. Rev. Lett. **97**, 150404 (2006).
[92] I. Prémont-Schwarz, A. Hamma, I. Klich, and F. Markopoulou-Kalamara, Lieb-Robinson bounds for commutator-bounded operators, Phys. Rev. A **81**, 040102(R) (2010).
[93] L. C. Venuti and P. Zanardi, Theory of temporal fluctuations in isolated quantum systems, Int. J. Mod. Phys. B **29**, 1530008 (2015).
[94] B. Zeng, X. Chen, D.-L. Zhou, and X.-G. Wen, Quantum information meets quantum matter, arXiv:1508.02595.
[95] K. Gregor, D. A. Huse, R. Moessner, and S. L. Sondhi, Diagnosing deconfinement and topological order, New J. Phys. **13**, 025009 (2011).
[96] A. Hamma, C. Castelnovo, and C. Chamon, Toric-boson model: Toward a topological quantum memory at finite temperature, Phys. Rev. B **79**, 245122 (2009).
[97] M. Serbyn, Z. Papic, and D. A. Abanin, Universal Slow Growth of Entanglement in Interacting Strongly Disordered Systems, Phys. Rev. Lett. **110**, 260601 (2013).
[98] Y. Zeng, A. Hamma, and H. Fan (unpublished).
[99] A. Pal and D. A. Huse, Many-body localization phase transition, Phys. Rev. B **82**, 174411 (2010).
[100] J. H. Bardarson, F. Pollmann, and J. E. Moore, Unbounded Growth of Entanglement in Models of Many-Body Localization, Phys. Rev. Lett. **109**, 017202 (2012).
[101] C. R. Laumann, A. Pal, and A. Scardicchio, Many-Body Mobility Edge in a Mean-Field Quantum Spin Glass, Phys. Rev. Lett. **113**, 200405 (2014).
[102] R. Nandkishore and D. A. Huse, Many-Body Localization and Thermalization in Quantum Statistical Mechanics, Annu. Rev. Condens. Matter Phys. **6**, 15 (2015).
[103] S. Suzuki, J. Inoue, and B. K. Chakrabarti, *Quantum Ising Phases and Transitions in Transverse Ising Models* (Springer, New York, 2013).
[104] A. P. Young and H. Rieger, Numerical study of the random transverse-field Ising spin chain, Phys. Rev. B **53**, 8486 (1996)
[105] V. Zatloukal, L. Lehman, S. Singh, J. K. Pachos, and G. K. Brennen, Transport properties of anyons in random topological environments, Phys. Rev. B **90**, 134201 (2014).
[106] B. Röthlisberger, J. R. Wootton, R. M. Heath, J. K. Pachos, and D. Loss, Incoherent dynamics in the toric code subject to disorder, Phys. Rev. A **85**, 022313 (2012).